A Hidden Dimension, Clifford Algebra, and Centauro Events

Carl Brannen*
A Quality Construction, Woodinville, WA†
(Dated: June 15, 2005)

This paper fleshes out the arguments given in a 20 minute talk at the Phenomenology 2005 meeting at the University of Wisconsin at Madison, Wisconsin on Monday, May 2, 2005. The argument goes as follow: A hidden dimension is useful for explaining the phase velocity of quantum waves. The hidden dimension corresponds to the proper time parameter of standard relativity. This theory has been developed into a full gravitational theory, "Euclidean Relativity" by other authors. Euclidean relativity matches the results of Einstein's gravitation theory. This article outlines a compatible theory for elementary particles.

The massless Dirac equation can be generalized from an equation of matrix operators operating on vectors to an equation of matrix operators operating on matrices. This allows the Dirac equation to model four particles simultaneously. We then examine the natural quantum numbers of the gamma matrices of the Dirac equation, and generalize this result to arbitrary complexified Clifford algebras. Fitting this "spectral decomposition" to the usual elementary particles, we find that one hidden dimension is needed as was similarly needed by Euclidean relativity, and that we need a set of eight subparticles to make up the elementary fermions. These elementary particles will be called "binons", and each comes in three possible subcolors.

The details of the binding force between binons will be given as a paper associated with a talk by the author at the APSNW 2005 meeting at the University of Victoria, at British Columbia, Canada on May 15, 2005. After an abbreviated introduction, this paper will concentrate on the phenomenological aspects of the binons, particularly as applied to the Centauro type cosmic rays, and gamma-ray bursts.

PACS numbers:

The paper consists of two sections. The first discusses binons, a subparticle postulated to make up quarks and leptons, and gives some details of their theory. The second discusses observational evidence for the existence of free binons.

I. A BRIEF INTRODUCTION TO BINONS

This first of two sections of this paper will give a brief introduction to binons. We begin with proper time and why it is natural to postulate a hidden dimension corresponding to proper time. Then we generalize the Dirac equation from an equation written in matrices and vectors to one written in matrices for both the operators and the wave. We extract the natural quantum numbers of the gamma matrices, and give the result for a general complexified Clifford algebra which will have a hypercubic form. We show that the quantum numbers of the fundamental fermions form a cube and postulate that the corners of the cube correspond to subparticles that make up quarks and leptons that we call "binons". We look at the quantum numbers of binons in detail. We postulate a simple potential function as the binding potential between binons. We discuss spin and statistics for binons as subparticles to quarks and leptons. We briefly discuss C, P, and T symmetry from the perspective of binons. We generalize the Space Time Algebra of David Hestenes[1] to a set of geometries more suited to the internal symmetries of particles, the Particle Internal Symmetry Algebra (PISA), which includes a hidden violation of Lorentz symmetry. We parameterize the various PISA geometries. We attribute the breaking of isospin symmetry to the PISA parameterization. Finally, we discuss spin in the context of a geometrization of particle internal symmetries.

A. Proper Time as a Hidden Dimension

In 1923, L. de Broglie proposed that matter possesses the same wave particle duality as light, with similar relations between frequency and energy.[2] As a consequence of time dilation and the relation $E = \hbar\omega$, [1] de Broglie concluded that there must be associated with a particle travelling at speed v, a wave that travels at (phase) speed:

$$v_\phi = \omega/k = c/\sqrt{1 - v^2} = c/\beta. \tag{1}$$

Since this speed is greater than c [3, P23.15], he referred to the wave as fictitous. The confusion was soon corrected when he realized that it is only the group velocity

*Electronic address: carl@brannenworks.com
†URL: http://www.brannenworks.com

[1] Some notation, for example the use of ω in preference to ν, has been changed to match modern usage.

that can be associated with the position of the particle, and the group velocity will be less than c.[2]

This has remained the conventional answer to this odd feature of the theory for the better part of a century. For example, in A. Messiah's excellent introduction to quantum mechanics, the details of the calculation for group velocity are given, but he fails to explicitly mention that the phase velocity exceeds c.[5, CH.II, §3] The paradox is not eliminated in relativistic quantum mechanics, though it is rarely mentioned. For example see [6, §3.3].

The presence of a hidden dimension, or multiple hidden dimensions, in Kaluza-Klein theories, as well as modern string theory, suggests that an explanation for the superluminal phase velocities of matter waves is that the wave is being considered in only 3 dimensions. A wave travelling with a phase velocity of c in 3 dimensions plus a hidden dimension, when translated into a wave in the usual space, will give a phase velocity in excess of c. This effect is commonly seen at the beach, where the velocity of breakers along the shore exceeds the velocity of the incoming waves. See Fig. (1) where the beach lies along the z axis, and we use s for the coordinate in the hidden dimension.

FIG. 1: Illustration of the increase in phase velocity when a hidden dimension is ignored. The true wavelength in 2 dimensions, λ, is increased to $\lambda_x = \lambda/\cos(\theta)$ when only the z dimension is considered. The phase velocity is $\lambda\omega/2\pi$.

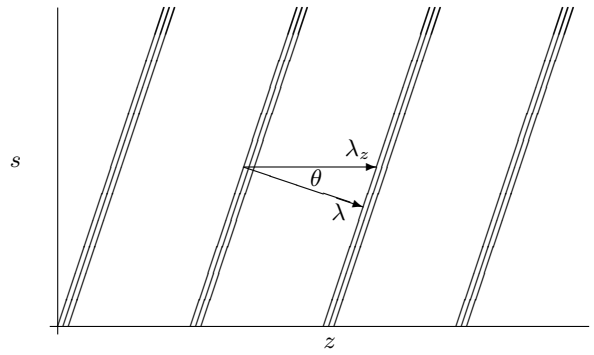

With the natural assumption that the true phase velocity of the matter wave is c, we can immediately derive a physical interpretation of the hidden dimension. Let $\psi(x, y, z, s, t)$ be a 5-dimensional plane wave travelling in the $+z$ direction:

$$\psi(x, y, z, s, t) = \psi_0(zk_z + sk_s - \omega t), \tag{2}$$

where k is the wave vector and ω is the frequency. In order to have a wave with a speed of c, we must have

$$c^2(k_z^2 + k_s^2) = \omega^2. \tag{3}$$

[2] For an interesting derivation of gravity in flat space-time from the optics of de Broglie's matter waves, see [4].

The phase velocity in the $+z$ direction is

$$v_\phi = c/\sqrt{1 - v_z^2/c^2} = \omega/k_z, \tag{4}$$

Squaring the second equality gives:

$$c^2k_z^2 = \omega^2(1 - v_z^2/c^2). \tag{5}$$

Subtracting this equation from Eq. (3) gives:

$$c^2k_s^2 = \omega^2(v_z^2/c^2). \tag{6}$$

Now our assumption was that the superluminal phase velocity of a de Broglie wave was due to the physical wave traversing a hidden dimension and possessing a true phase velocity of c. Under this assumption, the associated classical particle must also have a true velocity of c. In order for this to occur we must have:

$$c^2 = v_z^2 + v_s^2. \tag{7}$$

Substituting this relation into Eq. (6) puts it into the same form as Eq. (5):

$$c^2k_s^2 = \omega^2(1 - v_s^2/c^2). \tag{8}$$

Let us write the standard metric for special relativity with the proper time treated as a spatial dimension:

$$ds^2 = c^2\,dt^2 - (dx^2 + dy^2 + dz^2). \tag{9}$$

Dividing by dt^2 gives:

$$c^2 = \left(\frac{dx}{dt}\right)^2 + \left(\frac{dy}{dt}\right)^2 + \left(\frac{dz}{dt}\right)^2 + \left(\frac{ds}{dt}\right)^2 \tag{10}$$

Comparing with Eq. (7) shows that we must interpret v_s as ds/dt, and therefore the hidden dimension must be interpreted as corresponding to proper time. Keeping s as a spatial dimension, we will use the $(-++++)$ metric for space-time. That is, $g^{\mu\nu}$ is the diagonal matrix with entries $(-1, 1, 1, 1)$ or $(-1, 1, 1, 1, 1)$ depending on whether 4 or 5 dimensions are being discussed.

By assuming that nature keeps track of proper time with a hidden dimension, we explain several riddles related to the nature of our world. First, the coincidence that different reference frames agree on proper time intervals, while disagreeing about measurements of the usual spatial dimensions or time, is explained by the assumption that Lorentz boosts do not affect the proper time dimension. Second, that stationary matter contains large amounts of energy is explained by the assumption that stationary matter implicitly moves in a hidden dimension. Third, since we suppose here that matter always moves at the speed of light, it becomes obvious why we cannot arrange for it to exceed that speed in the usual 3 spatial dimensions. Fifth, our inability to measure the absolute phase of a quantum object can be seen to arise from our inability to measure absolute positions in the hidden dimension. Sixth, we can attribute the ability of matter to interfere with itself to interference over the

hidden dimension. Arranging for all quantum waves to travel at speed c promises to simplify quantum mechanics. Also, we can see reasons why Wick rotations have been so useful in quantum mechanics.

The use of a hidden dimension corresponding to proper time is neither unique nor original with this author, though this exposition, as far as I know, is. J. M. C. Montanus has published numerous articles which use the proper time of an object as its fourth coordinate.[7] He calls the result "absolute Euclidean spacetime" or AEST. The present work is distinguished from that of Montanus and similar work by others in "Euclidean relativity" such as A. Gersten [8], or [9] or the "4-dimensional optics" (4DO) of J. B. Almeida [10], or the "Gauge Theory of Gravity" [11–13] primarily in that this work will assume that the hidden dimension is cyclic and small. We will call this version of space-time the "proper time geometry" (PTG). For other work using proper time, see [14–16].

The above authors have mostly concentrated on showing that general relativity can be expressed in Euclidean coordinates. This paper will accept this conclusion and will concentrate on fitting elementary particles to this geometry.

When converting coordinates between classical relativity and the PTG, one simply ignores the s coordinate as it is infinitesimal in size. There will be a small error, but for a sufficiently small hidden dimension, the error will be below our capabilities for measurement. Examples of calculations in special relativity on the PTG are included in the Appendix A.

Given that the above authors differ from this one primarily in the assumption that the proper time dimension is cyclic and small, some defense of this position is required. First, the fact that the hidden dimension is hidden suggests that we should assume that it is small. Second, having a large hidden dimension corresponding to proper time requires that particles be able to collide despite having distinct values of proper time. Third, the weak force couples only to handed particles and handed particles travel at the speed of light. This is consistent with the fact that a cyclic hidden dimension as described here implies that speed in 3 dimensions is quantized, and the lowest energy particles would travel at speed c.

B. Generalizing the Dirac Equation

The crowning achievement of standard quantum mechanics is the calculation of the g-2 value for the electron to an accuracy of better than 10 decimal places. A theory claiming to be a unified field theory needs to be able to reproduce this calculation. The present theory will do this by deriving, from the principles of this theory, the propagators and vertices used in the Feynman diagrams of the standard model.

The derivation of the Dirac propagator from first principles will be given in a companion paper associated with the APSNW2005 meeting. This paper will restrict itself to deriving a few characteristics of the subparticles. But to see the necessity for these subparticles, it is useful to consider generalizations of the Dirac equation.

The usual massive Dirac equation allows the movement of a single spin-1/2 fermion to be modeled in a very precise manner. On the other hand, the standard model [17] attributes fermion masses as arising from exchange of Higgs bosons. Therefore it is the massless Dirac equations that are of interest. In this sense, the various elementary fermions all share the same Dirac equation, and this makes them distinct from the various elementary bosons. This suggests that it is natural to associate a distinct, but identical, Dirac equation with each type of elementary fermion.

An obvious way of obtaining a multiple particle massless Dirac equation is to leave the gamma operators alone, but to replace the spinors, with matrices. Each column of the matrix making up the multiparticle wave can be associated with a class of elementary fermion. For example, the first column could represent the electron, the second column the red down quark, the third column the green down quark, etc. The massless Dirac equation for the electron:

$$\left(\gamma_\mu \partial^\mu\right)_{4\times 4} \left(\psi_e\right)_{4\times 1} = 0, \tag{11}$$

where the gamma matrices satisfy

$$\gamma^\mu \gamma^\nu + \gamma^\nu \gamma^\mu = g^{\mu\nu}, \tag{12}$$

can be generalized to an equation for four fermions:

$$\left(\gamma_\mu \partial^\mu\right)_{4\times 4} \left(\psi_e, \psi_{dR}, \psi_{dG}, \psi_{dB}\right)_{4\times 4} = 0, \tag{13}$$

To separate the four components of the 4×4 wave matrix into the four different particles, one can use the projection operators: [3]

$$\eta_{00} = \begin{pmatrix} 1 & & & \\ & 0 & & \\ & & 0 & \\ & & & 0 \end{pmatrix} \quad \eta_{11} = \begin{pmatrix} 0 & & & \\ & 1 & & \\ & & 0 & \\ & & & 0 \end{pmatrix}$$
$$\eta_{22} = \begin{pmatrix} 0 & & & \\ & 0 & & \\ & & 1 & \\ & & & 0 \end{pmatrix} \quad \eta_{33} = \begin{pmatrix} 0 & & & \\ & 0 & & \\ & & 0 & \\ & & & 1 \end{pmatrix}, \tag{14}$$

where we use the notation η_{jk} to refer to the matrix with a one in the (i, j) location and the remainder of entries zero.

The four projection operators satisfy the following relations:

$$\begin{aligned} \eta_{jj}\ \eta_{kk} &= \delta^k_j\ \eta_{kk}, \\ \sum_k \eta_{kk} &= \hat{1}. \end{aligned} \tag{15}$$

---

[3] Mathematicians frequently refer to projection operators as "idempotents".

In addition, none of these projection operators can be written as a nontrivial sum of two other projection operators. This combination of attributes defines the four projection operators as a set of "mutually annihilating primitive idempotents".

Of course there are other sets of primitive idempotents for the 4×4 complex matrices. For example, if S is an invertible matrix, then $S\iota_k S^{-1}$ gives another set of primitive idempotents. But the particular set given above is significant because it projects the unified wave function $\Psi = (\psi_0, \psi_1, \psi_2, \psi_3)$ into distinct elementary fermions.

Thinking of the fermions in this manner promises to be useful in that it explains how it comes to be that linear combinations of fermions appear so often in the standard model. Therefore, to understand the symmetries of the fermions, we should examine the symmetries of the projection operators of the gamma matrices.

The association of the elementary particles with primitive idempotents is not an original idea of this paper. Most famously, J. Schwinger uses the same method in what is known as the "Schwinger measurement algebra". His analysis was devoted to kinematics instead of particle symmetries. For a brief introduction, see Appendix B.

C. The Quantum Numbers of a Complexified Clifford Algebra

Another reason for the utility of expanding the Dirac equation to operate on matrices instead of vectors is that one can then use the gamma matrices themselves as the basis for the matrices. There are sixteen different possible multiples of gamma matrices, other than sign differences, and these sixteen products provide a basis [6, §3.4] for 4×4 matrices over the complex numbers.

The four gamma matrices anticommute, so one can always reduce a product of gamma matrices to a product that contains no matrix more than once, and one can reorder the matrices to an appropriate standard. We will always assume that this is done, and furthermore we will abbreviate products of distinct gamma matrices as

$$\gamma^\mu \gamma^\nu = \gamma^{\mu\nu}. \tag{16}$$

As we later generalize to Clifford algebras, which is necessary in order to add the hidden dimension, s, we will abbreviate our notation and keep only the indices of the 5-vector of gamma matrices. For example,

$$\gamma^1 \gamma^2 = \gamma^{12} = \gamma^{xy} = \widehat{xy}. \tag{17}$$

Making this notation change will greatly ease our calculations, and it will more closely follow the mathematical literature, and in addition will make more clear the geometrical interpretation of our results.

The gamma matrices form a 4-vector so each individual gamma matrix is associated with a particular direction in space-time. Since any 4×4 matrix can be written as a sum over products [4] of gamma matrices, this gives us a geometric interpretation of any 4×4 matrix as a sum over complex multiples of products of geometric directions. When we extend spinors from vector form to matrix form, this extends the geometric interpretation of the components of 4×4 matrices to a geometric interpretation of the components of the spinors. Of course the geometric interpretation depends on the choice of representation of the gamma matrices.

Products of gamma matrices, like the matrices themselves, square to 1 or -1, so their eigenvalues will be ± 1 or $\pm i$. This is true for any of the products, but the products that are diagonal are particularly easy to analyze, so we will now choose a convenient representation. When we generalize to Clifford algebra, there will be no need to refer to any particular representation.

Since we expect that the chiral particles are fundamental, we will use a representation of the gamma matrices that has the left and right handed electron and left and right handed positron separated in the components of the usual spinor. In a later paper we will derive the massive Dirac propagator from the massless chiral propagators used here, but for now, we will simply treat the handed particles and antiparticles are distinct. The Weyl or chiral representation [6, §3.2] satisfies our requirements:

$$\hat{t} = \begin{pmatrix} 0 & 0 & 1 & 0 \\ 0 & 0 & 0 & 1 \\ 1 & 0 & 0 & 0 \\ 0 & 1 & 0 & 0 \end{pmatrix} \quad \hat{x} = \begin{pmatrix} 0 & 0 & 0 & 1 \\ 0 & 0 & 1 & 0 \\ 0 & -1 & 0 & 0 \\ -1 & 0 & 0 & 0 \end{pmatrix}$$
$$\hat{y} = \begin{pmatrix} 0 & 0 & 0 & -i \\ 0 & 0 & i & 0 \\ 0 & i & 0 & 0 \\ -i & 0 & 0 & 0 \end{pmatrix} \quad \hat{z} = \begin{pmatrix} 0 & 0 & 1 & 0 \\ 0 & 0 & 0 & -1 \\ -1 & 0 & 0 & 0 \\ 0 & 1 & 0 & 0 \end{pmatrix}. \tag{18}$$

The diagonal group elements are as follows:

$$\hat{1} = \begin{pmatrix} 1 & 0 & 0 & 0 \\ 0 & 1 & 0 & 0 \\ 0 & 0 & 1 & 0 \\ 0 & 0 & 0 & 1 \end{pmatrix} \quad i\widehat{xyzt} = \begin{pmatrix} -1 & 0 & 0 & 0 \\ 0 & -1 & 0 & 0 \\ 0 & 0 & 1 & 0 \\ 0 & 0 & 0 & 1 \end{pmatrix}$$
$$\widehat{zt} = \begin{pmatrix} -1 & 0 & 0 & 0 \\ 0 & 1 & 0 & 0 \\ 0 & 0 & 1 & 0 \\ 0 & 0 & 0 & -1 \end{pmatrix} \quad i\widehat{xy} = \begin{pmatrix} 1 & 0 & 0 & 0 \\ 0 & -1 & 0 & 0 \\ 0 & 0 & 1 & 0 \\ 0 & 0 & 0 & -1 \end{pmatrix} \tag{19}$$

Note that the above four elements are linearly independent and thus give a basis for the diagonal 4×4 matrices. Also note that we have included a factor of i so that these matrices each square to $\hat{1}$. When we generalize to Clifford algebra, we will use the "complexified" Clifford algebra so this can always be done.

---

[4] Since the gamma matrices anticommute, one can substitute commutation for multiplication in forming this group, provided one includes a factor of 0.5, for example see [6, §3.4]

It is also possible to do a similar analysis using real Clifford algebra. The idempotent structure of a Clifford algebra is referred, in the mathematical literature, to the "spectral basis" or "spectral decomposition" [18, pp201-2]. The real Clifford algebras are more complicated than the complexified ones because one can always multiply the basis vectors of a complexified Clifford algebra by i and so the signature does not matter much[5]. For simplicity, this paper will restrict itself to the complexified case with only one signature, and for familiarity we will use a geometry as similar as possible to the usual Minkowski.

When one is working with spinors, the effect of a choice of gamma matrix representation is to choose which components of the spinors are naturally separated. For example, one could choose the gamma matrices so that the four components of a spinor would correspond to electrons with S_{+x}, S_{-x}, and positrons with the same spin values. Since we are instead concerned with how the 4×4 matrix is broken into spinors, we instead look to which products of gamma matrices end up diagonal.

With the diagonal gamma products in this form, it's particularly easy to solve for the η_{kk} primitive idempotents in terms of gamma matrices. The results are:

$$\begin{aligned}
\eta_{00} &= (\hat{1} - \widehat{zt} + i\widehat{xy} - i\widehat{xyzt})/4 \\
\eta_{01} &= (\hat{1} + \widehat{zt} - i\widehat{xy} - i\widehat{xyzt})/4 \\
\eta_{02} &= (\hat{1} + \widehat{zt} + i\widehat{xy} + i\widehat{xyzt})/4 \\
\eta_{03} &= (\hat{1} - \widehat{zt} - i\widehat{xy} + i\widehat{xyzt})/4.
\end{aligned} \tag{20}$$

We can factor $\widehat{xyzt} = \widehat{xy}\widehat{zt}$ and put these into the more suggestive result:

$$\begin{aligned}
\eta_{00} &= (\hat{1} - \widehat{zt})(\hat{1} + i\widehat{xy})/4 \\
\eta_{01} &= (\hat{1} + \widehat{zt})(\hat{1} - i\widehat{xy})/4 \\
\eta_{02} &= (\hat{1} + \widehat{zt})(\hat{1} + i\widehat{xy})/4 \\
\eta_{03} &= (\hat{1} - \widehat{zt})(\hat{1} - i\widehat{xy})/4
\end{aligned} \tag{21}$$

This can be continued for the remaining η_{nm}, but the primitive idempotents are enough for this paper.

The four primitive idempotents η_{kk}, have the following eigenvalues with respect to the diagonal gamma matrix products:

	$\hat{1}$	$i\widehat{xy}$	$i\widehat{xyzt}$	$\widehat{zt}$
η_{00}	1	1	−1	−1
η_{11}	1	−1	−1	1
η_{22}	1	1	1	1
η_{33}	1	−1	1	−1

(22)

[5] For the case of real Clifford algebras, an interesting analysis of the signature issue is given by [19]. To see an analysis of the fermions for the general Clifford algebra case, both real and complexified, in various dimensions and signatures, see [20], where the signature and geometry choices of this paper are included as the second to the last line in the table showing symmetries towards the end of section II.

Of course $\hat{1}$ is a trivial operator, and $\widehat{zt}$ is simply the product of $i\widehat{xy}$ and $i\widehat{xyzt}$. Thus we can use the eigenvalues of $i\widehat{xy}$ and $i\widehat{xyzt}$ alone to define the η_{kk} primitive idempotents as shown in Fig. (2). Note that our choice of these two is somewhat arbitrary, we could instead have chosen $i\widehat{xy}$ and $\widehat{zt}$. The reason for making the choice given is so as to concentrate the directionality quantum numbers into just one factor.

FIG. 2: The natural primitive idempotents of 4×4 matrices plotted according to their eigenvalues with respect to the $\widehat{zt}$ and $i\widehat{xy}$ operators.

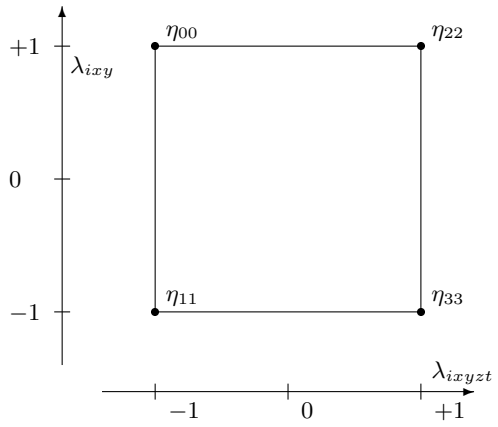

Fig. (2) shows that the quantum numbers of the gamma matrices form a square. This is a general attribute of Clifford algebras, namely that their quantum numbers form hypercubes[21, §17.5], also see [20].

The presence of hypercubes in the eigenvalue spectrum of Clifford algebras, along with the fact that Clifford algebras are the natural generalization of the Dirac gamma matrices, suggests that we should look for hypercubic symmetry in the elementary particles, a subject we will now turn to.

D. The Fermion Cube

The fermions in a family can be designated by their $\mathcal{SU}(2)$ and $\mathcal{U}(1)$ symmetry quantum numbers t_3 and t_0, or alternatively, by their electric charge Q and "neutral charge" (or "weak charge") Q'.[22, Table 6.2] The values for Q and Q' are related to t_3 and t_0 by

$$\begin{aligned}
Q &= t_3 + t_0, \\
Q' &= t_3 \cot(\theta_w) - t_0 \tan(\theta_w),
\end{aligned} \tag{23}$$

where θ_w is the Weinberg angle. We will use $sin^2(\theta_w) = 1/4$. A table of the usual quantum numbers for fermions is shown in Fig. (3). Values for antiparticles are the negatives of the values shown.

In Fig. (3), the alert reader will notice that we are using nonstandard notation for the electron and positron.

This is so as to bring all the fermions to the same standard. The antiparticles are written with a bar on top, the particles without. There is no need to indicate the electric charges as they are well known. In addition, there is no reason to show the electric charge while suppressing the neutral charge.

When the fermions are plotted according to their Q and Q' quantum numbers, the cubic nature of their symmetry is apparent. We will define the cube according to the n, l, and m vectors as shown in Fig. (4). The fact that the symmetry comes in cube form, rather than square, as we would be led to expect from the quantum numbers of the usual gamma matrices, indicates that our earlier expectation that there is a hidden dimension corresponding to proper time, s is vindicated. The hidden dimension expands the number of gamma matrices by one and this increases the dimensionality of their quantum numbers to cubic form.

In addition to the above mentioned deviation from standard notation, the alert reader will also note that we have deviated from standard practice in our designation of the handedness of the antiparticles. The standard model assigns handedness of the antiparticles in such a way that a spinor that corresponds to spin 1/2 for a particles gives spin $-1/2$ for the antiparticle. The standard model definition is compatible with the hole model of positrons. "If the missing electron had positive J_z, its absence has negative J_z".[6, Ch. 3.5] We will be modeling all particles on an equal footing. [6]

Both of the right handed neutrinos, ν_R and $\bar{\nu}_R$, end up at the origin, and we have to choose which goes with the visible part of the cube and which is hidden. Since the rest of the top part of the cube (i.e. $\{\bar{\nu}_L, \bar{e}_R, \bar{e}_L\}$) are all antiparticles, we will place the $\bar{\nu}_R$ with them. The n vector therefore runs in the direction from the $\bar{\nu}_R$ towards the e_R, the l runs towards the $\bar{e}_L$, and the m runs towards the $\bar{\nu}_L$.

FIG. 3: Table of standard model fermion quantum numbers.

	t_3	t_0	Q	$Q'\sqrt{3}/2$
e_R	0	-1	-1	1/2
e_L	-1/2	-1/2	-1	-1/2
ν_L	1/2	-1/2	0	1
ν_R	0	0	0	0
d_{*R}	0	-1/3	-1/3	1/6
d_{*L}	-1/2	1/6	-1/3	-5/6
u_{*L}	1/2	1/6	2/3	2/3
u_{*R}	0	2/3	2/3	-1/3

[6] Note that Fig. (4) suggests that the way that the standard model distinguishes between particle and antiparticle is arbitrary. In our model, for example, the up quark is a mixture of binons from a particle (neutrino) and binons from an antiparticle, (positron). Rather than the usual definition, a better definition of "antiparticle" is relational: the antiparticle of a binon is the binon opposite it in the fermion cube.

FIG. 4: The fermion cube. The ν_R is not shown for clarity.

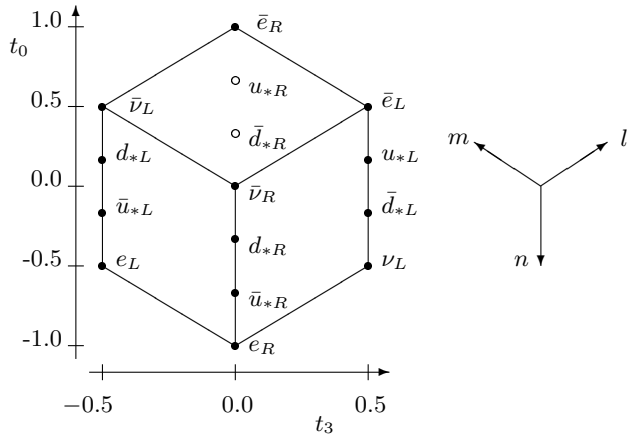

Fig. (4) shows that the leptons do have a cubic structure and can therefore be interpreted as primitive idempotents of a Clifford algebra. According to the illustrated choice of n, l, and m, and using the order $|n, l, m\rangle$, the assignments for the eight leptons are as follows:

$$\begin{aligned}
\bar{\nu}_R &\equiv |--\!-\rangle = |000\rangle = |0\rangle \\
\bar{\nu}_L &\equiv |--\!+\rangle = |001\rangle = |1\rangle \\
\bar{e}_L &\equiv |-+\!-\rangle = |010\rangle = |2\rangle \\
\bar{e}_R &\equiv |-++\rangle = |011\rangle = |3\rangle \\
e_R &\equiv |+--\rangle = |100\rangle = |4\rangle \\
e_L &\equiv |+-+\rangle = |101\rangle = |5\rangle \\
\nu_L &\equiv |++-\rangle = |110\rangle = |6\rangle \\
\nu_R &\equiv |+++\rangle = |111\rangle = |7\rangle
\end{aligned} \tag{24}$$

The multiplicity of the quarks, along with their intermediate positions between the leptons, suggests that each of the fermions is a composite particle composed of three subparticles, with the three subparticles possessing three different colors. Since the quantum numbers for a Clifford algebra can be described with binary numbers, we will call these subparticles "binons". See Fig. (5) for the composition making up a column of leptons and quarks. The column shown is the right most edge of the cube of Fig. (4).

A similar scheme for subparticles making up quarks and leptons is that of Harari[23], which differs from the present mostly in that this scheme treats the chiral fermions as the subparticles, rather than the fermions themselves. More complicated schemes abound, for example, [24].

In distinction from previous attempts at describing quark / lepton subparticles, we will provide a binding potential and give geometric derivations of the various particle symmetries. For an analysis of the requirements of color in Clifford algebras, especially noting that complexification is required, but not assuming that the quarks and leptons are composed of subparticles, see [25].

A weak force interaction, for example the conversion of

FIG. 5: A column of quarks and leptons shown as bound states of three binons each.

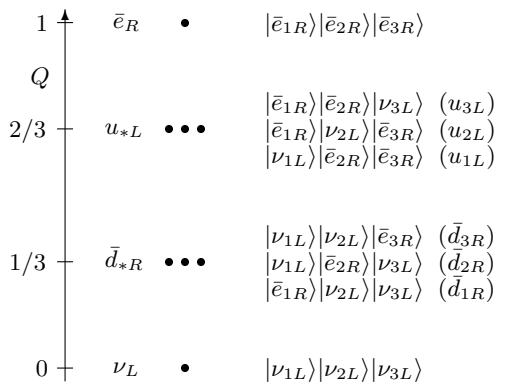

an electron to a neutrino, can be seen, in Fig. (5) to require the modification of all three binons comprising the electron. A strong force interaction, by contrast, requires only that two binons swap their positions. Thus the relative strength of the strong and weak force is likely due to the difference in the complexity of the binon interactions that comprise them.

E. Binon Quantum Numbers

As noted above, we must add a dimension in order to get a cube form for the binons. It is possible to add extra Clifford algebra vector basis elements without associating them with a hidden dimension, for example [26, 27], but this seems somewhat contrived, and we will instead only add one vector basis element to correspond to the hidden dimension corresponding to proper time. Adding this extra vector to the basis set for the gamma matrices is impossible with $4x4$ matrices, so we now pass to the more general Clifford algebra description.

Earlier, we concluded that space-time is a 5 dimensional mannifold with 4 spatial dimensions and one time dimension. One of the space dimensions, for which we will use the coordinate s, corresponds to proper time and is small and cyclic. We will use t for time, and x, y, and z for the usual spatial dimensions. The movement of particles is defined by the usual metric:

$$dt^2 = dx^2 + dy^2 + dz^2 + ds^2. \tag{25}$$

By the princpiles of Geometric Algebra[1, 28], there is a naturally associated Clifford algebra that is generated by vectors corresponding to these five coordinates, with a signature of $(-++++)$. With five basis vectors, there are then 32 different products that form the "canonical basis" for the Clifford algebra. These 32 products correspond to the 16 products of gamma matrices discussed earlier.

Since we are using a complexified Clifford algebra, we can always multiply canonical basis elements by i so as to arrange for their squares to be 1. Since physical operators need real eigenvalues, this will be convenient. With this modification, the 32 canonical basis elements are as follows:

$$\begin{array}{cccccc}
\hat{1} & i\widehat{x} & \widehat{xt} & i\widehat{xzs} & \widehat{yst} & i\widehat{yzst} \\
\hat{x} & i\widehat{xz} & \widehat{yt} & i\widehat{yzs} & \widehat{zst} & i\widehat{xyzst} \\
\hat{y} & i\widehat{xs} & \widehat{zt} & \widehat{xyt} & \widehat{xyzs} & \\
\hat{z} & i\widehat{yz} & \widehat{st} & \widehat{xzt} & i\widehat{xyzt} & \\
\hat{s} & i\widehat{ys} & i\widehat{xyz} & \widehat{xst} & i\widehat{xyst} & \\
i\hat{t} & i\widehat{zs} & i\widehat{xys} & \widehat{yzt} & i\widehat{xzst} &
\end{array} \tag{26}$$

Of the 32 canonical basis elements, Eq. (26) two, $\hat{1}$ and $i\widehat{xyzst}$ commute with everything. Since $\widehat{xyzst}$ squares to -1 and commutes with the whole algebra, it's natural to think of it as i, and most workers in Geometric algebra do just that.

Assigning $\widehat{xyzst} = i$ makes the interpretation of complex numbers geometric and this sort of thing common in work in the Geometric algebra.[29] Two exceptions are Almeida's insertion of $\mathcal{SU}(3) \times \mathcal{SU}(2) \times \mathcal{U}(1)$ symmetry into complexified Geometric algebra[30] and Avramidi's [31] generalization of the Dirac operator as a square root of the D'Alembert operator to Riemannian geometry.

Since this paper deals with both $\mathcal{SU}(3) \times \mathcal{SU}(2) \times \mathcal{U}(1)$ symmetry and uses a modification of the derivation of the Dirac equation to derive symmetry breaking, it is not surprising that this paper uses a complexified geometric algebra. While it is true that with the inclusion of the hidden dimension, the unit psuedoscalar, $\widehat{xyzst}$ squares to -1 and commutes with everything in the algebra, we will distinguish between $\widehat{xyzst}$ and i. However, it is clear that the two elements are difficult to distinguish and that this can be confusing, especially, as will be seen later in this paper, in the area of symmetry breaking.

The 31 nontrivial canonical basis elements all square to 1, and possess quantum numbers of ± 1. Any subset of them that commutes, and are not related trivially by multiplication, therefore provides a natural set of operators for the multiplicative quantum numbers of binons. Additive quantum numbers, in the physics literature, carry eigenvalues, at least for the fundamental particles, of ± 2 so the natural operators for those quantum numbers will be canonical basis elements divided by 2.

The distinction between additive and multiplicative quantum numbers need not concern us here. The only additive quantum number for a single binon that will possibly concern is is spin, and since we can simultaneously find eigenvectors of spin with particle type, we can, for the purpose of distinguishing individual binons, treat spin as a multiplicative quantum number. In fact, this turns out to be necessary for simplification.

With these basis elements, we can now begin the task of associating idempotents with the binons. In a sense, this is the Clifford algebra generalization of the choice of representation that we made for the gamma matrices, in that how we choose to write the idempotents, and therefore choose quantum numbers, corresponds to which

gamma matrices were chosen to be diagonal. Since we have an extra dimension, instead of choosing two gamma matrices diagonal, we now may choose three canonical basis elements (from the list in Eq. (26)), and these elements will define the quantum numbers that distinguish the binons. How we choose quantum numbers among the canonical basis elements is somewhat arbitrary. See AppendixC for a more general treatment.

One of the most important characteristics of a wave is the direction it is travelling in. We will want one of our quantum numbers to define the direction of travel in geometric terms. To determine this form, let $\psi(x,y,z,s,t) = \psi_{+z}(t-z)$ be a plane wave solution, of the massless Dirac equation in 5 dimensions, travelling in the $+z$ direction. Note that ψ_{+z} takes values among the Clifford algebra. Writing the Dirac equation in explicit geometric form and applying it to ψ gives:

$$\begin{aligned}(\hat{t}\partial_t - \hat{x}\partial_x - \hat{y}\partial_y - \hat{z}\partial_z - \hat{s}\partial_s)\psi_{+z}(t-z) &= 0\\ (\hat{t}+\hat{z})\psi_{+z} &= 0\\ (\hat{1}-\widehat{zt})\psi_{+z} &= 0, \end{aligned} \quad (27)$$

where the last equation is obtained by multiplying the previous by $-\hat{t}$. A general solution to Eq. (27) is:

$$\psi_{+z} = \frac{1}{2}(\hat{1}+\widehat{zt})\eta, \quad (28)$$

where η is an arbitrary Clifford algebraic constant, and the $1/2$ is included in order to make the $\hat{1}+\widehat{zt}$ into an idempotent. It is evident that the operator corresponding to movement in the $+z$ direction is given by $\widehat{zt}$, with eigenvalues of ± 1 corresponding to movement in the $\pm z$ directions.

Since our binons are to be interpreted as particles that move in various directions, we will choose $\widehat{zt}$ as a quantum number. More generally, for a particle travelling in the $\hat{v} = v_x\hat{x} + v_y\hat{y} + v_z\hat{z}$ direction, the appropriate operator will be $\hat{v}\hat{t}$.

We still have two more quantum numbers to pick. We would like the remaining quantum numbers to commute not only with $\widehat{zt}$, but to also commute with other possible choices such as $\hat{v}\hat{t}$. Otherwise more than just the one unavoidable quantum number will lose validity when we consider different directions of travel. This restriction greatly reduces the problem of defining the remaining quantum numbers. In order to commute with $\widehat{xt}$, $\widehat{yt}$ and $\widehat{zt}$, a canonical basis element will have to either avoid x, y, z and t, entirely or include them all. Eliminating unity, there are only three choices:

$$i\widehat{xyzt} \quad \hat{s} \quad i\widehat{xyzst} \quad (29)$$

We can take as our commuting operators $\widehat{zt}$ and any two of the above three.

Since these operators all commute, their various products will all possess simultaneous good quantum numbers. There are a total of eight such products:

$$\begin{array}{cccc} \hat{1} & \hat{s} & i\widehat{xyzt} & i\widehat{xyzst} \\ \widehat{zt} & \widehat{zst} & i\widehat{xy} & i\widehat{xys}. \end{array} \quad (30)$$

We can count the number of ways of assigning these to the n, l and m quantum numbers of Fig. (4). There are 7 choices for n and then 6 choices for l. For m, there are five left, but one of these is the product of n and l, so there are 4 choices. Thus there are 168 different assignments.

Once we have determined a correct solution for n, l and m, we can use the resulting quantum numbers to define the primitive idempotents associated with the binons. For example, if n l and m are the quantum numbers associated with the $\widehat{zt}$, $\hat{s}$ and $\widehat{xyzt}$ operators, then the eight binon idempotents are given by the generalization of Eq. (20):

$$(1 \pm \widehat{zt})(1 \pm \hat{s})(1 \pm i\widehat{xyzt})/8, \quad (31)$$

where each choice of the three $\pm$ defines one of the eight idempotents.

When we write down the binon binding potential we will find that energy will be minimized if certain idempotents are paired up with others. The patterns involved will greatly reduce the number of choices. The choices will be further reduced when we consider the manner in which the electron vs neutrino symmetry can be broken, but for now, let us move on to the binon binding potential.

F. The Binding Potential

It should be remembered that we complexified the Clifford algebra only under the interpretation that the complex phase would correspond to a rotation in the hidden dimension. The point here is that our use of complex numbers is for the sake of convenience in calculation only. Underlying this theory is a real valued geometric algebra in the tradition of Hestenes' work.[32] In our definition of the binon binding potential, we will therefore temporarily return to a real valued Clifford algebra.

Let three binons be given the real valued wave functions $\psi_1(r)$, $\psi_2(r)$, and $\psi_3(r)$, where $r = (r_x, r_y, r_z, r_s)$ defines a position in space. The definition of the potential that we will use will be the simplest function possible:

$$V = V_0 \int |\psi_1 + \psi_2 + \psi_3|^2 d^4r, \quad (32)$$

where V_0 is a positive real constant, and $|\ \ |^2$ is defined as the usual norm for a Clifford algebra:

$$|\sum \alpha_\chi \hat{\chi}|^2 = \sum |\alpha_\chi|^2, \quad (33)$$

where $\hat{\chi}$ is a canonical basis element, the α_χ are real numbers, and the sum runs over all 32 (real) $\hat{\chi}$ values. For example,

$$|\hat{x} + 5\hat{y} + 10\widehat{xyzs}|^2 = 126. \quad (34)$$

Consider one of the real canonical basis elements, for example, $\hat{\chi}$. Let the phases of ψ_1, ψ_2 and ψ_3 be given

by δ_1, δ_2 and δ_3. Then in real terms, the values of the $\hat{\chi}$ components of ψ_n are:

$$\begin{aligned}\mathcal{R}(\alpha_{n\chi}(s)) &= |\alpha_{n\chi}| \cos(s+\delta_n) \\ &= \beta_n \cos(s+\delta_n), \end{aligned} \tag{35}$$

where β_n is the magnitude of the complex number $\alpha_{n\chi}$ and δ_n is the phase. The integral over s is easily evaluated to give:

$$\begin{aligned} & V_0 \int |\alpha_{1\chi}(s) + \alpha_{2\chi}(s) + \alpha_{3\chi}(s)|^2 ds, \\ = \; & V_0 \int |\beta_1 \cos(s+\delta_1) + \beta_2 \cos(s+\delta_2) + \beta_3 \cos(s+\delta_3)|^2 ds, \\ = \; & \pi V_0 |\beta_1 e^{i\delta_1} + \beta_2 e^{i\delta_2} + \beta_3 e^{i\delta_3}|^2, \\ = \; & \pi V_0 |\alpha_{1\chi} + \alpha_{2\chi} + \alpha_{3\chi}|^2, \end{aligned} \tag{36}$$

where we have taken the s dimension to run from 0 to 2π. We will remove the factor of π by taking it into V_0. Thus we see that complexifying the Clifford algebra had the effect of simplifying our potential energy calculation by allowing us to use complex numbers to emulate rotations in the hidden dimension. We replace the integral over 4 spatial dimensions in Eq. (32) with an integral over the usual 3 spatial dimensions of the complex wave functions:

$$V = V_0 \int |\psi_1 + \psi_2 + \psi_3|^2 dx\, dy\, dz, \tag{37}$$

For the chiral fermions, we will assume that the wave functions are the lowest energy possible, so that as far as dependence on position goes, each of the ψ_n is an identical Gaussian. By making this assumption, we need not consider the spatial parts of their wave functions.

Obviously we can minimize this potential by arranging for $\psi_1+\psi_2+\psi_3 = 0$ everywhere. That is, we could assign the exact same idempotent to each of the three binons, and arrange their phases so that the sum cancelled. This would be in violation of the spirit of the Pauli exclusion principle, so it is clear that in order to obtain realistic solutions, we must require that the combined wave function of a group of binons be antisymmetrical under the exchange of two binons.[33, CH. XIV]

The three binons making up a single chiral fermion can only be distinguished by arranging for them to have differing directions. On the other hand, the chiral fermion they make up has a preferred direction, that is, the direction of its spin and / or its direction of travel. The component of velocity of the binon in the direction of travel of the chiral fermion has to be c, so the binon must be travelling faster. Therefore we will assume that the binons are tachyonic particles.[7]

[7] For a phenomenological approach to the situation of different particles possessing different maximum velocity (effective speeds of light), in the context of high energy cosmic rays see [34]. Also see [35] which proposes that tachyonic neutrinos are responsible for the knees in the cosmic ray spectrum.

For a comment on tachyons and quantum mechanics, in particular how Lorentz symmetry is altered, see [36]. For a paper on Lorentz symmetry violations at high energies in general, see [37]. Having neutrinos travel at other than c could be a part of neutrino mixing according to [38]. For an extensive and recent review of Lorentz violation in theory and experiment, see [39] which has 202 references.

This paper does not postulate a violation of Lorentz symmetry for normal matter. What it does instead is to postulate that subparticles flagrantly violate Lorentz symmetry, but that their bound states achieve exact (to within experimental error) Lorentz symmetry. Consequently, the absence of experimental detection of Lorentz symmetry violation in normal matter is not of concern here.

This paper's approach to tachyons is different from the usual unstable or false vacuum seen in QFT.[40] We will assume that the true speed of waves is faster than c, and that chiral fermions and photons are composite particles that is restricted to travelling at speed c. The chiral fermions then combine to produce massive fermions that move at speeds less than c. There are thus two levels of combination, each associated with a reduction in speed.

In order to allow color to be an unbroken symmetry, it is natural to expect that the three binons travel at the same angle with respect to the fermion. Let that angle be θ_B. Then the relative speeds of the particles is given by:

$$c_B = c/\cos(\theta_B). \tag{38}$$

The three binons travel on a cone centered on the fermion velocity / spin vector. The opening angle of the cone is θ_B. The three binons are arranged equidistantly around the cone. See Fig. (6).

FIG. 6: Direction vectors for the three binons making up a fermion. The fermion vector is marked e. The binons are marked R, G and B. $\angle R0e = \angle G0e = \angle B0e = \theta_B$. $\angle ReG = \angle GeB = \angle BeR = 120$ degrees.

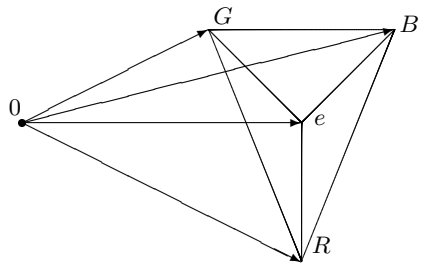

Having the binons travel faster than c is compatible with the assumptions of the version of general relativity

associated with this theory. Euclidean relativity defines a coordinate system similar to that of Newton, and in such a preferred rest frame, there is no causality problem with travelling faster than c.

For other examples of tachyonic particles and preferred frames, see [41]. An entertaining review of tachyons is [42]. Also see [43, 44]. Also see M. Consoli and E. Costanzo's[45] reopening of the historical conclusions of the Michelson-Morley experiments.

A perhaps less radical alternative to the assumption of tachyonic binons would be to suppose that they carry fractional spin. While fractional spin, and the case of spin-1/6 in particular, has been explored in string theories[46], the match with experimental observation is better with tachyonic binons, and the theory is easier to derive from standard quantum mechanical principles.

For now, let us note that for normal energies and unexotic matter (and even, apparently, some exotic matter), the tachyonic nature of binons is hidden by their being bound into composite particles, and the next subsection will discuss further the question of the relationship between binons and fermions.

G. Spin and Statistics

The operators $\{i\widehat{yz}, -i\widehat{xz}, i\widehat{xy}\}$ form a representation of $\mathcal{SU}(2)$, and so can be thought of as the spin operators, $\{\sigma_x, \sigma_y, \sigma_z\}$. Since $i\widehat{xy}$ is included in the list of good quantum numbers for a particle moving in the $+z$ direction Eq. (30), it is true that a binon travelling in the $+z$ direction does possess, individually, a good quantum number that corresponds to spin in the z direction. But the three binons making up a fermion cannot point in the same direction as the fermion, and the binons individually are not spin-1/2 particles. This is a subtle point that is easy to overlook and bears comparison with the usual situation.

The spinor that represents a particle of spin-1/2 has two complex degrees of freedom. An assembly of three such particles has a total of eight degrees of freedom. An elementary exercise in quantum mechanics is to convert between the representations of the spinors of the individual particles and the spinor of the combination using Clebsch-Gordon coefficients. The Clebsch-Gordon series can be written as:

$$\begin{array}{ccccccccccc} 2 & \times & 2 & \times & 2 & = & 4 & + & 2 & + & 2' \\ |\frac{1}{2}\rangle & \times & |\frac{1}{2}\rangle & \times & |\frac{1}{2}\rangle & = & |\frac{3}{2}\rangle & + & |\frac{1}{2}\rangle & + & |\frac{1}{2}\rangle' \end{array} \tag{39}$$

On both sides of the equation there are eight complex degrees of freedom, two in each of the spin-1/2 spinors, and four in the spin-3/2 spinor. The spinor multiplication forms a tensor product. The usual Clebsch-Gordon coefficients give the conversion with respect to a particular spin axis, for example S_z. That is, when each of the seven spinors in the above are written in their S_z basis, the Clebsch-Gordon coefficients give the conversion from one side to the other.

The three binons making up a fermion have only one complex degree of freedom each. Rather than spin-1/2, fermions, as far as degrees of freedom go, the binons are non commutative spin-0 fermions. Consequently, the Clebsch-Gordon series for three binons combining to form a chiral fermion is trivial:

$$\begin{array}{ccccccc} 1 & \times & 1 & \times & 1 & = & 1 \\ |0\rangle & \times & |0\rangle & \times & |0\rangle & = & |0\rangle \end{array} \tag{40}$$

where the three particles on the left are written in three different bases, that is, they are written as idempotents according to their direction of travel.

The binons are made up of a nondirectional part, for example, $(1+i\widehat{xyzt})(1-\hat{s})$, and a part which, under spatial rotations, acts as a scalar plus a vector for example, $(1+\widehat{zt})$. A more complete derivation of the spinor nature of fermions as binon bound states will be provided in a later paper, which will also derive the Dirac propagator and derive certain mass relations amongst the fermions.

If the binons did commute, which would be the case if they were travelling in the same direction, when one applied antisymmetrization to the combined wave function one could only obtain zero. But the noncommutativity of the binons allows one to apply antisymmetrization to the wave function for a collection of three of them. In addition, if the binons did travel in the same direction, if one were to mix two different types of binon to form a quark, one would find that since distinct idempotents annihilate each other, the antisymmetrization would give zero.

In order to compute the antisymmetrization of the binon wave function, let us begin by aligning the spin / velocity axis of the chiral fermion with the $(\hat{x}+\hat{y}+\hat{z})/\sqrt{3}$ vector. By choosing to have the fermion aligned in the $(1,1,1)$ direction, we can arrange for the R binon to be oriented in the direction of the x axis, the G to be oriented in the direction of the y axis, and the B to be oriented in the direction of the z axis.

With the angle θ_B, the idempotents corresponding to these three binons are then:

$$\begin{aligned} \eta_R &= (\widehat{xt}+\widehat{yt}+\widehat{zt})\frac{c_B}{\sqrt{3}}+(2\widehat{xt}-\widehat{yt}-\widehat{zt})\frac{s_B}{\sqrt{6}} \\ \eta_G &= (\widehat{xt}+\widehat{yt}+\widehat{zt})\frac{c_B}{\sqrt{3}}+(2\widehat{yt}-\widehat{zt}-\widehat{xt})\frac{s_B}{\sqrt{6}} \\ \eta_B &= (\widehat{xt}+\widehat{yt}+\widehat{zt})\frac{c_B}{\sqrt{3}}+(2\widehat{zt}-\widehat{xt}-\widehat{yt})\frac{s_B}{\sqrt{6}}, \end{aligned} \tag{41}$$

where c_B, s_B are cosines and sines of θ_B. Note that the above equations have left off the nondirectional part of the idempotent. Since the directional parts commute with the nondirectional parts, the nondirectional parts, all being identical, do not contribute to the antisymmetrization, though they do contribute to how the result of the calculation acts as an eigenvector of S_{x+y+z}.

Referring back to Eq. (31), it is clear that each of our idempotents will have a real term of value 1/8. In order to get these terms to cancel, we must have that the three binons have complex phases that add to zero. Of

course the only three complex phases that add to zero are multiples of the cubed roots of unity:

$$1, \;\; u = \exp(+2i\pi/3), \;\; \text{and} \;\; u^* = \exp(-2i\pi/3). \quad (42)$$

These phases will be used so frequently that we will use u and u^* to signify two cube roots of unity.

If we take the η_R, η_G and η_B to be multiplied by 1, r and s, respectively, then, in addition to their real terms, all their nondirectional terms, which include the upper half of the good quantum number operators listed in Eq. (30), will be cancelled out of the complex sum:

$$\eta_R + u\eta_G + u^*\eta_B. \quad (43)$$

This is due to the fact that these nondirectional terms are identical between the idempotents, and are not altered by the differences in direction. In addition, by symmetry, this is a solution to the problem of minimizing the potential energy of the η_n over the possible choices of phase for each.

According to the antisymmetrization postulate, the combined wave function for the binons (after cancelling u factors) will be given by:

$$\begin{aligned} \eta \;\; &= \;\; \eta_R\eta_G\eta_B + \eta_G\eta_B\eta_R + \eta_B\eta_R\eta_G \\ &- \;\; \eta_R\eta_B\eta_G - \eta_G\eta_R\eta_B - \eta_B\eta_G\eta_R. \end{aligned} \quad (44)$$

In the above, the right hand side will be a function of θ_B.

We expect that the combined wave function will be an eigenfunction for spin. Upon performing the calculation, it turns out that this can only happen if $\cos(\theta_B) = 1/3$. [8] Accordingly, for the remainder of this paper we will take the value of θ_B to be $\cos^{-1}(1/3) = 70.528$ degrees. For this particular angle, the results of the anticommutation program is:

$$-6i(1 + \hat{v}\hat{t})\ \iota\ /\sqrt{27} \quad (45)$$

where $\hat{v} = (\hat{x} + \hat{y} + \hat{z})/\sqrt{3}$, and ι is the nondirectional part of the idempotents.

Before antisymmetrization, the three binons broke the radial symmetry around the $(1, 1, 1)$ direction. That is, while the particle as a whole was oriented in the $(1, 1, 1)$ direction, there was one binon each oriented in approximately in the x, y and z directions. But as a result of the antisymmetrization, the wave function corresponding to the bound state, Eq. (45), no longer has any orientation but that of $(1, 1, 1)$. This is consistent with experimental observation that electrons have only a single axis of orientation.

For $cos(\theta_B) = 1/3$, the directional parts of η_R is:

$$\eta_R = (5\hat{x}\hat{t} - \hat{y}\hat{t} - \hat{z}\hat{t})\iota/\sqrt{27}. \quad (46)$$

The results for η_G and η_B are similar, with x, y and z cyclically permuted.

The value of the potential at $\cos(\theta_B) = 1/3$ works out to be:

$$V = V_0|(\frac{\widehat{xt}}{\sqrt{3}} + \frac{\widehat{yt}u^*}{\sqrt{3}} + \frac{\widehat{zt}u}{\sqrt{3}})\iota|^2 = 0.25. \quad (47)$$

The potential energy for a single binon is $V_0 8 \times (1/8)^2 = V_0/8$, so the binding potential is only 1/3 of the total energy of the system. This is another way of saying that a chiral lepton, while containing 33% less energy than a naked binon, is still an extremely energetic particle, as will be discussed in the next section.

One might expect that $cos(\theta_B) = 1/3$ if one were to suppose that the binons each carry spin $\hbar/2$, but at an angle so as to attribute each binon as contributing $\hbar/6$ to the total fermion spin.

This paper associates the elementary particles with the idempotents rather than the nilpotents of the Clifford algebra. This is somewhat contrary to expectations in that the Grassmann algebra used for fermions in QFT consists of nilpotents. However, the antisymmetrization assumption is sufficient to arrange for products of identical fermions to give zero. [9]

H. Quarks

An antisymmetrization procedure was used in the previous subsection to derive leptons as composed of three identical binons with different directional orientations. The same antisymmetrization procedure, when applied to the possible bound states made from three non identical binons forces the elimination of all exotic combinations leaving only the quarks.

Consider a mixture of three non identical binons. As before, write them as primitive idempotents with a single directional idempotent, which we will label with the colors as η_{1R}, η_{2G} and η_{3B}, and a nondirectional component, which is colorless and which we will call ι_1, ι_2 and

[8] Other values for θ_B give a result of the form $\kappa(1 + \beta i\widehat{xy})$ where $\beta \neq 1$. It may be possible to interpret these as eigenvectors of a spin operator more general than ones constructed from the Clifford algegbra. In doing so, one would bring back the usual quantum distinction between operators and eigenvectors.

[9] If you use the idempotent/nilpotent structure of a Clifford algebra to separate a nonlinear wave equation into linear (Dirac) equations and nonlinear interactions, then you find that, in general, the linear equations for the propagation of the idempotents and nilpotents have a different speed. Idempotents cannot bind together when sharing the same direction, but nilpotents, particularly after symmetry breaking, may be able to. However, the speed of such bound nilpotents may not be equal to the free speed of the idempotents.

ι_3. The three idempotents are thus:

$$\begin{aligned} \eta_R &= \iota_{1R}\,\iota_1, \\ \eta_G &= \iota_{2G}\,\iota_2, \\ \eta_B &= \iota_{3B}\,\iota_3. \end{aligned} \tag{48}$$

When we perform products of the above three idempotents, note that any single directional component, such as ι_{1R}, commutes with all the nondirectional components, ι_1, ι_2 and ι_3. Thus any product can be split into a product of directional and nondirectional idempotents:

$$\begin{aligned} \eta_R\eta_G\eta_B &= \iota_{1R}\,\iota_1\,\iota_{2G}\,\iota_2\,\iota_{3B}\,\iota_3, \\ &= (\iota_{1R}\,\iota_{2G}\,\iota_{3B})(\iota_1\,\iota_2\,\iota_3). \end{aligned} \tag{49}$$

Since the nondirectional idempotents, ι_1, ι_2 and ι_3 are members of the same set of primitive idempotents, they are self annihilating. Thus the product will be zero unless all three nondirectional idempotents are identical. On the other hand, the directional idempotents are based on three different directions. The self-annihilating property does not apply to them. Therefore, the only possible mixed states of three binons will occur as mixtures of binons that are identical except for a directional quantum number. This is precisely the structure shown in Fig. (4).

It is a fairly easy task to write a computer program to look for bound states between mixtures of binons. One finds that if it were not for the antisymmetrization principle (or even a principle that only required that the products of the bound binons be nonzero) one would have large numbers of exotic bound states. Not only do the quarks show up as bound states, their binding energy is higher than the leptons. These binding energies are still almost unimaginably high. In addition, the binding energies for the chiral fermions has nothing to do with their masses, which we will discuss next.

I. Lepton Generations and Masses

We will use the exmaple of the electron in this subsection, along with the muon and tau, but the principles apply to the other fundamental fermions and their antiparticles. This subsection is intended only as a brief introduction, a more complete description of the theory will await the next paper.

An electron is composed of two chiral halves, e_R and e_L. As in the old zitterbewegung model, these two move at speed c and transform from one to the other.

In the present theory, the e_L and e_R are each composite particles composed of three binons each. In order for an e_R to transform to an e_L, each of its three binons must transform.

We will compute the transition probabilities for binons using the traditional quantum mechanical principle that the probabilities are proportional to the squared magnitude of the inner product of the two states being transformed between.

This rule for transition probabilities will allow a binon of one color to transform to a different color. This means that a colorless particle, such as an electron, does have a probability of turning into a colored particle. Of course it will immediately turn right back for energetic considerations.

The act of transforming from one state to another is similar to the act of wave function collapse in that it happens at a point in space. While color is not conserved, position will be, and in particular, the position in the hidden dimension will be conserved. Since we are modeling the position in the hidden dimension with complex phases, this means that when a binon transforms from one state to another, it will have to preserve its phase.

Were it not for the issue of complex phases, we could model the sequence of transformations of a binon with a Markov chain. The addition of complex phases implies that an appropriate transition matrix will have probabilities multiplied by complex phases. Since there are three colors of binons, the complex transition probability matrix will be 3×3.

For a solution to the problem of propagating in such a way that a particle is stable, we will look for the eigenvectors of the transition probability matrix. There will be three such eigenvectors and they will correspond to the three generations of fermions. Their associated eigenvalues will give their respective masses. In our next paper we will derive some surprising relationships between fermion masses from these principles.

Since color is not conserved by binon interactions, a colored high energy particle, upon collisions with normal matter, will have a branching ratio to transform into a combination of particles that are colorless. This effectively confines color.

The fact that binons group together in 3s to form normal matter, along with pair production of binons and the ability of binons to transform amongst themselves, suggest that a single free binon, upon colliding with normal matter, will first combine with two other binons to form a fermion. The other binons involved will combine similarly.

J. The Particle Internal Symmetry Algebra

The binon model of the elementary particles is based on an assumption that the internal symmetries of the particles can be given geometric meaning in terms of basis vectors that have very specific meaning in the usual world. Only the proper time vector, $\hat{s}$, would be entirely unfamiliar to a geometry student of ancient Egypt.

In this primitive framework, the complexities of the standard model of quantum mechanics are difficult to envisage. Under our assumptions, we expect to find the symmetries of our apparently Lorentz symmetric world repeated in the structure of the elementary particle interactions, but the elementary particle interactions are not nearly so symmetric as Lorentz symmetries.

Weak hypercharge has a $\mathcal{U}(1)$ symmetry, which can be represented by a single complex number. Weak isospin has $\mathcal{SU}(2)$ symmetry and is represented by a spinor. The Weinberg angle, θ_W, determines the relative strength of the weak and electromagnetic forces in terms of weak hypercharge and weak isospin. Thus these two symmetries, weak hypercharge and weak isospin, are intimately related in the structure of the standard model.

Any spin$-1/2$ fermion has a spin axis, a $3-$vector that defines a direction that its spin always gives $+\hbar/2$ when measured along. This suggests that a geometric representation of spin should be accomplished by an object that can be thought of as a vector, (or axial vector). According to the theory of relativity, space and time are intimately related, so whenever we have a spatial $3-$vector, it must be part of a $4-$vector with the missing component corresponding to time.

That there is, in the standard model, no $4-$*vector* whose spatial components give the spin axis of a particle suggests that the internal symmetries of the particles are not Lorentz symmetric. If the internal symmetries were Lorentz symmetric, then we would expect a very particular relationship between spin and its time component. Later in this paper we will devote a subsection to deriving, from geometric principles, that the time component of spin is helicity.

The relationship between weak hypercharge, which is a $\mathcal{U}(1)$ symmetry, and weak isospin, which is an $\mathcal{SU}(2)$ symmetry also suggests a violation of Lorentz symmetry in the internal states of particles. Here, neither of the symmetries is apparently connected to space-time, but in a geometric theory based on a generalization of the Dirac equation, it is inevitable that weak hypercharge will be associated in some way with time, while weak isospin will be associated in some way with space.

For both the spin / isospin $4-$vector, and the weak hypercharge / weak isospin relationship, we need to look for ways to violate Lorentz symmetry in the internal symmetries of our theory. But at the same time, we must retain Lorentz symmetry in terms of matching the results of the standard model.

A typical calculation for quantum mechanics is given in terms of Feynman diagrams. These diagrams consist of propagators and vertices. The propagators for fermions arrange for the particles to obey the Dirac equation. If, when we break Lorentz symmetry, we can do it in such a way as to leave the Dirac equation unmodified, then all we need do, to obtain the same results as the standard model, is derive the vertex values.

If we were still working with a Dirac equation that only dealt with a single spinor, we would be stuck. But since our Dirac equation has been generalized, we can consider modifications to it that mix the spinors in a non Lorentz symmetric manner, but leave each spinor still satisfying a standard Dirac equation. Since we are treating mass as a particle interaction, we need only do this operation on the massless Dirac equation:

$$(\hat{t}\partial_t - (\hat{x}\partial_x + \hat{y}\partial_y + \hat{z}\partial_z + \hat{s}\partial_s))\psi = 0. \tag{50}$$

This paper has already assumed a version of general relativity that suggests a preferred, Euclidean, rest frame. It has further assumed binons that travel at speed $3c$, an assumption that demands a preferred rest frame. It should not shock the reader that we will now promote the speed of light from a scalar to a Clifford algebraic constant.

While doing this, we will want to leave the Clifford algebraic structure unaltered. Suppose that c_α satisfies the following commutation relations [10]:

$$\begin{aligned}
\hat{t}c_\alpha &= c_\alpha\hat{t},\\
\hat{x}c_\alpha &= c_\alpha^{-1}\hat{x},\\
\hat{y}c_\alpha &= c_\alpha^{-1}\hat{y},\\
\hat{z}c_\alpha &= c_\alpha^{-1}\hat{z},\\
\hat{s}c_\alpha &= c_\alpha^{-1}\hat{s}.
\end{aligned} \tag{51}$$

Under these restrictions, it is easy to verify that the five elements (note that they are no longer vectors):

$$\hat{t},\ c_\alpha\hat{x},\ c_\alpha\hat{y},\ c_\alpha\hat{z},\ c_\alpha\hat{s}, \tag{52}$$

satisfy the same relations as the usual basis vectors of a Clifford algebra (or the gamma matrices of the Dirac equation). For example,

$$\begin{aligned}
(c_\alpha\hat{x})^2 &= c_\alpha\hat{x}c_\alpha\hat{x} &(53)\\
&= c_\alpha c_\alpha^{-1}\hat{x}^2\\
&= 1\\
(c_\alpha\hat{x})(c_\alpha\hat{y}) &= c_\alpha c_\alpha^{-1}\hat{x}\hat{y} &(54)\\
&= -c_\alpha c_\alpha^{-1}\hat{y}\hat{x}\\
&= -(c_\alpha\hat{y})(c_\alpha\hat{x})\\
(c_\alpha\hat{x})\hat{t} &= -c_\alpha\hat{t}\hat{x} &(55)\\
&= -\hat{t}(c_\alpha\hat{x}).\\
& &(56)
\end{aligned}$$

Therefore, the asymmetric Dirac equation:

$$(\hat{t}\partial_t - c_\alpha(\hat{x}\partial_x + \hat{y}\partial_y + \hat{z}\partial_z + \hat{s}\partial_s))\psi = 0, \tag{57}$$

can in no way be distinguished from the usual symmetric one Eq. (50). In terms of the mathematics of the algebras they define, they are both the same Clifford algebra, and are as indistinguishable as different representations of the gamma matrices.

While our use of the asymmetric Dirac equation is no change from the usual Dirac equation in terms of Clifford

---

[10] The commutation relations, in addition to allowing a modification of the Clifford algebra canonical basis vectors in a way that preserves the Clifford algebra structure, also happen to be precisely the modifications that can be made to the Dirac equation spatial components so as to retain it as a square root of the unmodified Klein-Gordon equation. This is how the author first discovered these relations as well as the parameterization shown in the next subsection.[47]

algebra, it does mark a departure from the Dirac equation of Hestenes' geometric algebra. What we have done is to modify the definition of the spatial vectors so as to give them what will turn out to be the form of mixed vectors. At the same time, we will persist in thinking of these vectors in terms of the tangent vectors of the space-time manifold. We will call the resulting algebra for space-time, the Particle Internal Symmetry Algebra, or PISA.

Up to now, all our work has been with the Geometric algebra. We need some tools to allow conversion between solutions to Geometric algebra and PISA wave equations. Such a tool will allow us to make difficult PISA computations using easy Geometric algebra techniques.

Let ψ_S be a solution to the usual Dirac equation Eq. (50). Assuming that c_α has a square root and that the square root satisfies the same commutation relations given in Eq. (51), we can calculate as follows:

$$\begin{aligned}
(\hat{t}\partial_t - (\hat{x}\partial_x + \hat{y}\partial_y + \hat{z}\partial_z + \hat{s}\partial_s))\psi &= 0, \\
c_\alpha^{0.5}(\hat{t}\partial_t - (\hat{x}\partial_x + \hat{y}\partial_y + \hat{z}\partial_z + \hat{s}\partial_s))c_\alpha^{-0.5}c_\alpha^{0.5}\psi &= 0, \\
(\hat{t}\partial_t - c_\alpha^{0.5}c_\alpha^{0.5}(\hat{x}\partial_x + \hat{y}\partial_y + \hat{z}\partial_z + \hat{s}\partial_s))(c_\alpha^{0.5}\psi) &= 0, \\
(\hat{t}\partial_t - c_\alpha(\hat{x}\partial_x + \hat{y}\partial_y + \hat{z}\partial_z + \hat{s}\partial_s))(c_\alpha^{0.5}\psi c_\alpha^{-0.5}) &= 0.
\end{aligned} \tag{58}$$

Therefore, if ψ_S is a solution of the usual Dirac equation, then a solution to the PISA Dirac equation is given by:

$$\psi_A = c_\alpha^{0.5}\psi_S c_\alpha^{-0.5}. \tag{59}$$

If ψ_S is written as a primitive idempotent, for example:

$$\psi_S = (1+e_1)(1+e_2)(1+e_3)/8, \tag{60}$$

then ψ_A will also be a primitive idempotent, but with modified operators:

$$\psi_S = (1+c_\alpha^{0.5}e_1c_\alpha^{-0.5})(1+c_\alpha^{0.5}e_2c_\alpha^{-0.5})(1+c_\alpha^{0.5}e_3c_\alpha^{-0.5})/8. \tag{61}$$

The modified primitive idempotent will operated on by the modified operator, will possess the same quantum numbers that the unmodified idempotent had when operated on by the unmodified operator. For example:

$$\begin{aligned}
e_1(1-e_1) &= -(1-e_1), \\
c_\alpha^{0.5}e_1c_\alpha^{-0.5}(1-c_\alpha^{0.5}e_1c_\alpha^{-0.5}) &= -(1-c_\alpha^{0.5}e_1c_\alpha^{-0.5})
\end{aligned} \tag{62}$$

In general, making the change from Geometric algebra to PISA will not modify any relation that is based on multiplication or addition of Clifford algebraic numbers. However, our definition of the inner product used an absolute value, and therefore will be modified. Eventually we will associate probabilities with the inner product, so these probabilities will change. And modifications of the binon binding potential will determine which binons can bind together to form composite objects made of mixed binons such as the quarks.

If an operator has an even number of spatial components, then it will be unmodified in the conversion from GA to PISA. Otherwise, it will be multiplied on the left by c_α. For example:

$$\begin{aligned}
c_\alpha^{0.5}\hat{t}\alpha^{-0.5} &= \hat{t} \\
c_\alpha^{0.5}\hat{x}\alpha^{-0.5} &= c_\alpha\hat{x} \\
c_\alpha^{0.5}\widehat{xt}\alpha^{-0.5} &= c_\alpha\widehat{xt} \\
c_\alpha^{0.5}\widehat{xy}\alpha^{-0.5} &= \widehat{xy} \\
c_\alpha^{0.5}\widehat{xyt}\alpha^{-0.5} &= \widehat{xyt} \\
c_\alpha^{0.5}\widehat{xyz}\alpha^{-0.5} &= c_\alpha\widehat{xyz}
\end{aligned} \tag{63}$$

In the next subsection, we will derive the solutions to the c_α commutation relations, parameterize these solutions in a convenient way, and establish some useful relations.

K. PISA Parameterization

Write c_α as a sum over canonical basis elements:

$$c_\alpha = c_1\hat{1} + c_x\hat{x} + ... + c_{xyzst}\widehat{xyzst}, \tag{64}$$

where c_χ is a complex number. According to Eq. (51), c_α must commute with $\hat{t}$ and with any even product of spatial vectors. This requirement forces all but four of the c_χ coefficients to be zero. The remaining coefficients are:

$$c_\alpha = c_1\hat{1} + c_t\hat{t} + c_p\widehat{xyzs} + c_c\widehat{xyzst}, \tag{65}$$

where we have shortened the names of three of the coefficients. Two of these are identical to the four good nondirectional quantum numbers, but the other two are not.

From Eq. (51) we have that $(c_\alpha\hat{x})^2 = \hat{1}$. Putting Eq. (65) in and comparing terms gives four equations:

$$\begin{aligned}
\hat{1}\,(c_1c_1 - c_tc_t + c_pc_p - c_cc_c) &= \hat{1}, \\
\hat{t}\,(c_1c_t - c_tc_1 + c_pc_c - c_cc_p) &= 0, \\
\widehat{xyzs}\,(c_1c_p - c_tc_c - c_pc_1 + c_cc_t) &= 0, \\
\widehat{xyzst}\,(c_1c_c - c_tc_p - c_pc_t + c_cc_1) &= 0.
\end{aligned} \tag{66}$$

These reduce to give the equations relating the coefficients as:

$$\begin{aligned}
c_1^2 - c_t^2 + c_p^2 - c_c^2 &= 1, \\
c_1c_c - c_tc_p &= 0,
\end{aligned} \tag{67}$$

the other two equations giving $0 = 0$. Since we have two equations in four unknowns, the solution set can be parameterized with two free parameters.

Let c_α be given as follows:

$$c_\alpha(\alpha_t, \alpha_s) = \exp(i\alpha_t\hat{t})\exp(\alpha_s\widehat{xyzs}). \tag{68}$$

We now show that $c_\alpha(\alpha_t, \alpha_s)$ so defined satisfies the commutation relations and is therefore the parameterized solution to Eq. (67)

Since $\hat{t}$ and $\widehat{xyzs}$ commute, we have that:

$$\exp(i\alpha_t\hat{t} + \alpha_s\widehat{xyzs}) = \exp(i\alpha_t\hat{t})\ \exp(\alpha_s\widehat{xyzs}), \quad (69)$$

and therefore,

$$\exp(-i\alpha_t\hat{t} - \alpha_s\widehat{xyzs}) = 1/\exp(i\alpha_t\hat{t} + \alpha_s\widehat{xyzs}), \quad (70)$$

Since $\hat{t}$ commutes with $i\alpha_t\hat{t} + \alpha_s\widehat{xyzs}$, we have that $c_\alpha(\alpha_t, \alpha_s)$ commutes with $\hat{t}$. Since $i\alpha_t\hat{t} + \alpha_s\widehat{xyzs}$ anti-commutes with $\hat{x}$, we have:

$$\exp(i\alpha_t\hat{t} + \alpha_s\widehat{xyzs})\hat{x} = \hat{x}\exp(-i\alpha_t\hat{t} - \alpha_s\widehat{xyzs}).$$

This completes the verification that $c_\alpha(\alpha_t, \alpha_s)$ satisfies the commutation relations Eq. (51).

Summing up, a set of useful equations involving $c_\alpha(\alpha_t, \alpha_s)$ are:

$$c_\alpha(\alpha_t, \alpha_s)^n = c_\alpha(\alpha_t n, \alpha_s n), \quad (71)$$
$$c_\alpha(\alpha_t, \alpha_s)\ \hat{u} = \hat{u}\ c_\alpha^{-1}(\alpha_t, \alpha_s), \quad (72)$$
$$c_\alpha(\alpha_t, \alpha_s)\ \hat{t} = \hat{t}\ c_\alpha(\alpha_t, \alpha_s), \quad (73)$$

where $\hat{u}$ is any spatial vector.

L. The Time Component of the Spin Vector

In the standard model, spin is a vector operator, and it remains so in this theory:

$$\mathbf{S} = (S_x, S_y, S_z) = (i\widehat{yz}, -i\widehat{xz}, i\widehat{yz}). \quad (74)$$

The special theory of relativity uses $4-$vectors instead of treating space and time separately. It therefore is natural to ask what the time component of the spin vector is. Similarly, in this geometric theory, time is treated on an equal footing with the spatial directions, so given a spatial vector, it is possible to find a more or less unique time component associated with it.

In the special theory of relativity, a Lorentz boost mixes the space and time components of a $4-$vector. However, a Lorentz boost on a (Pauli) spinor, has only the effect on the spinor of rotating the vector associated with the spinor. The same effect happens with the four component bispinors of the Dirac theory.[6, §3.3] From the principles of relativity, one would expect that the three spatial components of the vector associated with the spinor would be mixed with the time component of the spinor.[48]

In theories where there is a preferred reference frame, which includes the "Lorentz Ether Theory" that Einstein's relativity replaced [49] this discrepancy in the use of spinors in the standard model is not a surprise. Instead, the Lorentz symmetry is assumed to be accidental[11], so no assumptions about the internal symmetries of the particles can be made from it.

[11] For an interesting note on how Lorentz symmetry can appear naturally in a physical system without relativity, see [50]

To derive the time component of spin, we begin by first converting spin from an axial vector into vector form by multiplying by $-\widehat{xyz}$. In vector form, the time component is obtained by replacing the spatial vector basis elements with $\hat{t}$. Then we convert back by multiplying by $\widehat{xyz}$ to give the time component in axial vector form:

$$\begin{pmatrix} i\widehat{yz} \\ -i\widehat{xz} \\ i\widehat{xy} \\ ? \end{pmatrix} -> \begin{pmatrix} i\hat{x} \\ i\hat{y} \\ i\hat{z} \\ i\hat{t} \end{pmatrix} -> \begin{pmatrix} i\widehat{yz} \\ -i\widehat{xz} \\ i\widehat{yz} \\ -i\widehat{xyzt}. \end{pmatrix} \quad (75)$$

The time component of spin is $\pm i\widehat{xyzt}$, where the sign is somewhat arbitrary. We will take the positive sign. This can be written as $i\widehat{xy}\ \widehat{zt}$, which is the product of the operator for spin in the z direction, and the operator for velocity in the z direction. This is therefore the helicity operator.

An analysis of the bound states of binons will provide insight into such diverse subjects as the mass relations of the leptons and the generalized Cabibbo angles. The brief introduction included here is enough to establish the general properties of binons as is needed for the observational section of this paper.

II. HIGH ENERGY COSMIC RAYS & C.

This section will include a brief description of the facets of high energy cosmic rays and related astronomical oddities that may be explained by binons. In addition to high energy cosmic rays in general, we will cover the mysterious Centauro and Chiron events, gamma ray bursts, galactic jets and the GZK limit.

A. Extreme High Energy Cosmic Rays

While the composition and behavior of most cosmic rays are well understood, extremely high energy cosmic rays exhibit behavior which is difficult to understand. There are several excellent reviews of the problem. For an extensive and recent review of high energy cosmic rays, see [51]. For a review concentrating on potentials for new physics, see [52].

The most interesting data for high energy cosmic rays comes form film or emulsion based ground targets. This data is frequently ignored in reviews of high energy cosmic rays, such as the two mentioned above, as they are of considerably smaller energies, but there is much more detailed information for these events, and they are strange. For an in depth review with plenty of data on these events see [53], which the reader is urged to obtain. For a brief review of Centauros from the point of view of accelerator physics, see [54]. We will include here a brief description of these unusual events.

Anomalous events on emulsion and film have now been unexplained for three decades. From a recent review article:

> The most striking, unexpected phenomena observed in emulsion chamber experiments are Centauro events with an exceptionally small number of photons, events with particles or groups of particles being aligned along a straight line, halo events characterized by an unusually large area of darkness in the X-ray film, and deeply penetrating cascades. Whether these phenomena are related to fluctuations and the measurement technique of emulsion chamber experiments or signs of new physics is controversially debated for more than 30 years.[55]

The term "Centauro" refers to a cosmic ray that exhibits an anomalous ratio of charged to neutral pion production. This is a violation of isospin symmetry. In the standard model only the weak force violates isospin symmetry, so one would expect that Centauro events are collisions mediated by the exchange of a weak vector boson. However, Centauros exhibit cross sections that are even larger than strong force cross sections for protons.

Theoreticians have come up with plenty of possible explanations for the odd behavior of high energy cosmic rays. Causes include correlations in production of pions[56, 57], "disordered chiral condensates"[58] or "quark gluon plasma"[53], highly energetic goldstone bosons[59], strangelets[60], or evaporating black holes[61].

The $\pi^{\pm}/\pi^0$ ratio is measured by relying on the fact that π^0s quickly decay into photons. Thus the particle shower initiated by a π^0 consists, at least at first, of gamma-rays, electrons and positrons. These "electromagnetic" particles are quickly absorbed in relatively thin layers of matter. On the other hand, a $\pi^{\pm}$ produces a shower of hadrons which are much more penetrative.

The electromagnetic part of a shower is detected by the uppermost layer of the cosmic ray target, while its deeper layers detect the hadron rich $\pi^{\pm}$ portion.

For a typical cosmic ray event, the size of the electromagnetic shower and the hadron shower are approximately equal. It was the absence of an electromagnetic shower in the presence of a very strong hadron shower that caught the attention of the Brazil-Japan cosmic ray collaboration at Chacaltaya.[62, 63] They named the event "CentauroI" in allusion to the mismatching of the top and bottom parts of a Centaur.

In addition to the Centauros, other high energy cosmic ray events appear to be balanced in their hadronic / electromagnetic components, but contain particles with larger than expected penetrability. In addition, these events tend to be aligned on the target to an extent greater than that predicted by QCD. These events are called "Chirons".

If a Centauro event were to occur at high altitude, the particle showers produced would degrade by the time they penetrated the remainder of the atmosphere, with the hadrons producing electromagnetic showers and the electromagnetic particles producing hardonic showers. It would therefore be difficult or impossible to distinguish the ratio of neutral to charged pions. It is generally believed that such a Centauro event would be classified as a Chiron.

Because of the thickness of the atmosphere, most potential Centauros will begin at high altitude, and consequently will be classified as something other than "Centauro" when their tracks are observed. In fact, Chirons are observed at a rate of about 0.1 per square meter per year, while Centauros are about 10 to 100 times less frequent, at the Chacaltaya altitude.[53]

The debris from a Chiron is spread around by the time it reaches the target. Typically, there will be a number of "mini-clusters". Each mini-cluster is thought to be the particle shower that results from a collision by the primary particle. The mini-clusters are frequently aligned, and they indicate a high level of transverse momentum, p_T. The fact that mini-clusters tend to be aligned suggests that all the miniclusters are produced in a single collision.

The cosmic ray emulsion experiments that are the most extensive in surface area are the ones that are most likely to observe Centauros. Unfortunately, the more extensive experiments typically have less target depth and consequently can give less information about how the Centauro primary particles interact with matter. Since Centauros are known to be deeply penetrating particles, these experiments can do little to measure the true total energy of a Centauro.

Very thick lead targets with many layers of emulsion are most suited at measuring cross sections, energy and momenta of high energy cosmic rays, but since these targets are small in surface area, they are unlikely to see any low altitude, and therefore clean, Centauro showers. Instead, what they typically see are mixed showers of particles from high altitude primary collisions.

As a result of these material limitations, our data on high energy cosmic rays is split between fairly good energy, momentum and cross section data about the particles resulting from high altitude collisions, for which we can know little about the $\pi^{\pm}/\pi^0$ ratios, and low altitude collisions with good ratios but poor energy and cross section data. And these cosmic rays are only a fraction of the energy of the largest cosmic rays seen, which are detected at long distance by their air showers rather than by emulsion or film.

B. Anomalous Transition Curves

With each collision with an atom of atmosphere or target, the cosmic ray particle produces a shower of debris. With time, or equivalently, with distance, the shower grows until its energy is converted to particles that do not interact much. The resulting curve, called a "transition curve", gives the size of the shower as a function of its depth. Transition curves for a single shower look more or less like an upside down parabola, with the max-

imum of the parabola corresponding to the depth where the shower reached its maximum energy deposition.

After developing the film in a cosmic ray experiment, the experimenters measure the transition curves by measuring the amount of exposure to the film or by counting the number of particle tracks in emulsion. As a primary particle travels through the detector, each collision it has with a target particle produces new particle showers, each with its own transition curve. The result is a series of bumps in the energy deposition graph, with one bump corresponding to approximately one collision.

Chirons produce odd transition curves in that they, as well as some of the collision products that produce, sometimes penetrate quite deeply. In addition, their transition curves sometimes fail to decrease much with depth. A transition curve for a typical Chiron that fully penetrates a deep lead chamber is sketched in Fig. (7).

FIG. 7: Sketch of a transition curve showing Chiron type anomalies in deep lead cosmic X-ray film. This is a sketch only, for real data see [53]. The horizontal axis is depth, in cascade units. The vertical axis is the log of the number of tracks. In this case, the primary particle exits through the bottom of the detector after 11 collisions. There are two anomalies in this sort of transition curve. First, the particle is extremely penetrative. Second, the distance between collisions is too short for a typical hadron to be the primary particle.

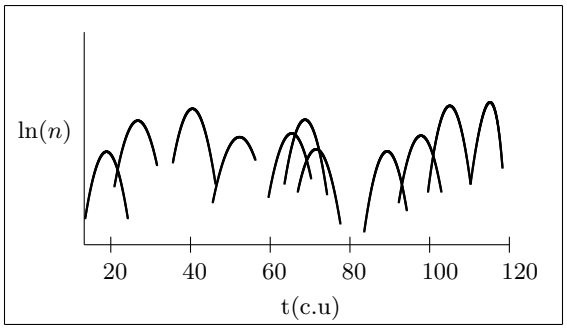

Since ultra high energy cosmic rays are not generally seen emerging from the earth, it is clear that Chirons must eventually be absorbed by normal matter. Every now and then, this is observed in deep lead chambers. For example, see PB73 Block8 S127-100 shown in Figure 2.16 of [53]. In such a case, the primary particle will cease colliding somewhere above the bottom of the detector. A sketch of a typical case is shown in Fig. (8). About half of all mini-clusters exhibit unusually high penetrative ability.[53]

The high rate at which Chiron fragments collide can be illustrated by comparing the geometric mean free path in the target with the collision mean free path for the cosmic ray particles. The Chirons are able to travel only about 1/2 as far as the geometric mean free path would indicate. This is shown by examining the distribution of the position of the first shower in a Chiron mini-cluster.[53,

FIG. 8: Sketch of a Chiron type transition curve anomaly in which the primary particle disappears inside the detector. In this case, the particle has 6 collisions in the first half of the detector.

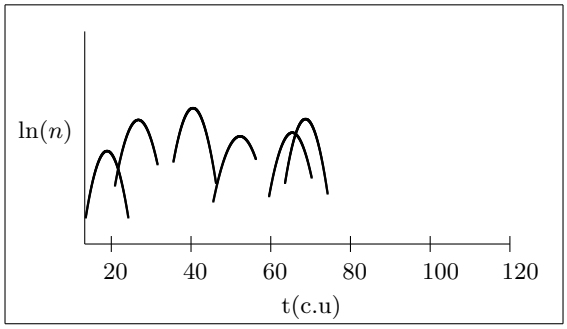

Fig. 2.13]

The geometric mean free path that the mini-cluster data gives are compared with that of typical low energy cosmic rays, which are mostly protons. If mini-clusters are the results of high altitude collisions of the cosmic ray primary, they are expected, in the standard model, to be hadrons generally smaller than protons. That the collision mean free path for the mini-clusters is less than that of the proton is therefore particularly unexpected.[53]

C. High Transverse Momementum

The transverse momentum of mini-clusters in Chiron events is computed using the formula:

$$p_T = E\, r \,/\, h, \tag{76}$$

where E is the energy of the mini-cluster, r is the measured offset of the mini-cluster from the center of the event, typically a few mm, and h is the height at which the collision occured, typically a kilometer. For most Chiron events, h is estimated by assuming a figure for the magnitude of p_T. For a few, the height can be estimated by triangulation of the particle paths.

Since the mini-clusters are themselves made up of hadrons, the same equation can be applied to the hadrons of the mini-cluster itself. When one does this, however, the evidence from the mini-clusters suggests much lower values of h, and therefore much higher values of p_T than QCD can account for.[54] The value of $E\,r$ between mini-clusters is about 300 times as large as the value inside a given mini-cluster.[53]

The low transverse momentum of the debris in a mini-cluster is what we expect from an extremely relativistic air shower. What is anomalous is the very high transverse momentum in the primary collision. The conflict suggests that the primary collision (or collisions) were not governed by Lorentz symmetry, as we will propose later in this paper.

D. Alignment and Multiplicity

The mini-clusters of Chiron events have a tendency to be aligned to a degree in excess of that predicted by QCD. For an extensive discussion of the alignment issue of Centauro events, with simulations of what would be expected, see [64]. For a discussion of alignment in a particularly clean high altitude Centauro, see [65]. Also see [66]. Since the alignment occurs between mini-clusters, it is clear that alignment is part of the problem of excessive transverse momentum.

If the primary for a Chiron were a heavy nucleus, as would explain the high cross section and penetrability, we would expect to see a large number of fragments in the initial collision at high altitude. Each of these fragments, which would be called "jets" in accelerator language, would produce its own mini-cluster. The number of mini-clusters, or "multiplicity", therefore, suggests an obvious way of deducing the complexity of the primary cosmic ray.

If the primary for a Chiron were even as large as a proton, then we would expect to see a fairly large number of jets. It would be natural for these to be aligned, as jets tend to be coplanar. However, about half of Chirons include only a single mini-cluster, which is sometimes called a "uni-cluster". This suggests that these Chirons must be simple particles.

Occassional Chirons are observed with extremely high numbers of mini-clusters, but these are believed to be the result of air degradation of a parent collision with 4 or 5 particles. For the standard model of QCD, the problem here is that the low multiplicity of some Chiron events is incompatible with the high transverse momentum and alignment of the high multiplicity events.

Mini-clusters that have passed through a sufficient amount of atomsphere appear to degrade into a "halo", which describes a region of the film where a large amount of energy is deposited more or less evenly over a wide region. Halos are difficult to analyze in terms of total energy deposited, but they appear to be hadron rich.[53] The presence of halos gives clear evidence that the low transverse momentum of mini-clusters is due to the extreme speed of the particle generating the mini-cluster shower, rather than some effect which collimates the debris of an air shower.

E. Jets, Quasars, & c.

The other half of the Centauro question is where they come from. The film based cosmic ray targets, given the rotation of the earth, give only limited indications of what direction these cosmic rays arrive from, beyond "up". A useful experiment would be to combine a film based cosmic ray target with a cosmic ray detector that is sensitive only to high energy cosmic rays, and that would give an indication of the time of arrival of a Centauro. In addition, the experiment would give an idea of the time duration of a Centauro, as compared to more usual cosmic ray showers as will be later discussed.

If there were astronomical sources of Centauros, we would expect to see particle showers when these sources interact with matter. Such a particle shower would be recognizable because it would be, like the Centauro air showers themselves, extremely energetic and very well collimated.

In fact, astronomers do observe highly relativistic "jets". Some of these jets are extragalactic and are associated with quasars or the centers of other galaxies.[67, 68] A variet of quasar known as a "blazar" exhibits extremely fast variation in intensity. The cause of the variation, as well as the source of jets in general, is still mysterious though the relation with "active galactic nuclei" that are responsible for quasars is now clear.[69–71]

In addition to the nuclei of galaxies, including our own, there are also small relativistic jets present around our own galaxy. These are associated with black holes, neutron stars or x-ray binaries. These sources, because of their similarity to quasars, are sometimes called "microquasars".[72] Microquasars are also associated with gamma-rays.[73]

Relativistic jets, when observed from small angles with respect to their direction of propagation, will sometimes appear superluminal. This easily explained effect is from the geometry only, and has nothing to do with the tachyonic nature of binons.

F. Gamma-Ray Bursts

If an astronomical jet is caused by Centauros, the resulting particle shower will include a lot of charged particles that will be diverted by magnetic fields. However, there will also be gamma-rays, and some of these may have energies low enough to survive the journey to the earth still pointing back towards their source.

Every now and then, very large numbers of high energy gamma-rays hit the earth, all from the same direction. These are called gamma-ray bursts (GRB). Gamma-ray bursts are sometimes followed by delayed bursts from the same direction. A delay as long as 77 minutes has been observed, and this is difficult for models to explain, mostly due to the fact that the delayed burst is not thermal, though there are some efforts.[74]

In addition to delayed bursts, GRB are also afflicted with precursor activity that is difficult to explain. Precursors have been found up to 200s before the main burst (the longest time searched), and possessing non-thermal, softer spectrums than the main burst:

> We have shown that a sizable fraction of bright GRBs are characterised by weak but significant precursor activity. These precursors have a delay time from the main GRB which is surprisingly long, especially if compared to the variability time scale of the burst

itself. The precursor emission, contrary to model predictions, is characterised by a non-thermal spectrum, which indicates that relativistic electrons are present in the precursor emission region and that this region is optically thin.[75]

G. The GZK Limit

In the 1960s, soon after the discovery of the cosmic microwave background, Greisen, Kuzmin and Zatsepin realized that protons and neutrons would encounter the cosmic microwave background as high energy gamma rays, would scatter off it with production of pions, and would consequently slow down. This should result in a cutoff in the spectrum of cosmological cosmic rays at just below 10^{20}eV. For protons of energy 10^{20} to 10^{21}eV, the attentuation length is of order a few Mpc.[76]

Because of the GZK limit, there are proposals that high energy cosmic rays are generated in the cosmological neighborhood[77] or are from the creation of charged black holes[78]. These proposals fail to give any hint as to why the Centauro events are anomalous.

A similar argument to the GZK limit has been put forward in [79] to argue that the speed of light is very close to the maximum speed that a material body can achieve. These arguments do not apply to a subparticle that may not possess an electric charge. For an article on Cherenkov radiation emitted by superluminal particles, see [80].

Gonzalez-Mestres argues that evidence for extreme tachyons, (i.e. $c_i \gg c$) might be seen in cosmic rays[81] and that this could be an explantion for the evasion of the GZK limit.[82] Also see [83] for a discussion of small differences in particle speeds allowing the GZK cutoff to be broken.

It has been suggested that ultra high energy cosmic rays could be associated with quasars, provided that one avoids the GZK limit by assuming a "messenger" particle that does not interact with photons.[84, 85] Given the evidence from emulsion and film targets, this assumption is natural. The classical Centauro produced very few photons in its debris, so one would expect that it would have a very low cross section for collisions with photons.

Cosmic rays are always more numerous at lower energies. If one draws a curve showing the number of cosmic rays seen at energies from the lowest to the highest, the curve drops off at about E^{-3}. Accordingly, it is customary to plot frequency multiplied by energy cubed. The approximate shape of the curve is shown in Fig. (9). The presence of the ankle suggests that the particles responsible for Centauro events either evade the GZK cutoff or are produced fairly locally, but whether or not the ankle exists is still being debated.[87]

FIG. 9: The "ankle" of the cosmic ray flux.[86] Flux values are given by $log(Flux * E^3)$ in units of $eV^2m^{-2}s^{-1}/sr$. Energy is given by $log(E)$ in units of eV. The ankle begins at around $E = 10^{19}eV$, and is shown as a thin line due to its uncertainty.

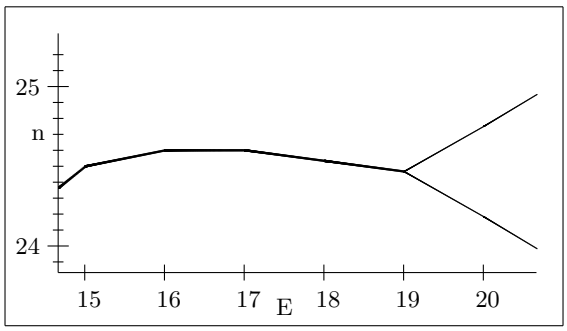

III. SIGNATURES OF FREE BINONS

We expect that free binons would be extremely rare, but it is not unlikely that some have already been observed. This section compares what we would expect of binons to the various astronomical puzzles reviewed in the previous section.

A. Elastic Binon Collisions and Mini-Clusters

Since binons are supposed to underly both the weak and strong forces, it is natural that they interact more strongly than the strong force, but still violate isospin symmetry. This combination is an attribute that specifically defines the Centauro events.

Consider a binon travelling in the $+z$ direction that collides with a electron or quark. Since we are here considering the possibility that binons are responsible for Centauro events, and we suspect that the primary particles responsible for these events do not interact much with photons, we will assume that the binon is one of the neutrino type binons.

The collision will involve 4 binons. There is some chance that there will be an elastic collision, in the sense that the result will give one free binon and another quark or fermion.

Since the collision products of such an elastic collision travel at different speeds (that is, the binon is tachyonic while the normal matter is not), the binon will separate from the normal matter particle shower. When the binon later produces a normal particle shower, the two showers will arrive in reverse order. That is, the first normal particle shower will arrive last.

The separation of the normal particle shower from the binon will have observable consequences. First, the particle shower will be spread out in time. Second, the movement of the tachyonic particle does not obey Lorentz symmetry, and so must be analyzed in the preferred rest

frame.

If, in the preferred rest frame, the target has motion perpendicular to the binon, then the particle showers for the later collisions of the binon will arrive at different times, and therefore at different positions on the target.

For example, if the binon has two elastic collisions, and then is converted into normal matter, there will be a total of three separate particle showers produced. In the preferred rest frame, relativistic effects will cause these three showers to be closely collimated and they will travel down the same path.

However, if the target is moving in the preferred reference frame, the three showers will hit the target at three different points. Furthermore, the three points where the showers hit will tend to be aligned. Therefore, we will expect to have aligned showers despite each shower being extremely relativistic. The effect will be a series of aligned particle showers, just as is seen in the Chiron events. We will assume that each elastic binon collision produces a new mini-cluster.

From the alignment data for Chirons, along with an estimate of the speed of the earth against the preferred reference frame, we can estimate the distance between elastic binon collisions, as well as the attentuation length for binons converting into normal matter in the high atmosphere.

Not very many physicists believe in a preferred reference frame, so estimates of the earth's movement through it have not received as much attention as one might desire. Arbitrarily, we will use Consoli's figure of about 200km/s.[45] Ignoring the orbital motion of the earth, the average perpendicular motion of the earth in the preferred reference frame will be about $\pi/4$ of this or 160km/s.

According to [64], the average radius of aligned 4-core events is 1.8cm, which gives a total diameter of 3.6cm, or 1.2cm for the collision length. At 150km/s, this gives a time delay between particle showers of an average of 80ns. Assuming that $\theta_B = \cos^{-1}(1/3)$, this gives a distance between collisions of about 50m.

A distance of 50m seems small, except when you consider the possibility that the binons that are impinging on the earth are not necessarily the same as the ones resulting from the "elastic" collisions discussed here. Since Centauros are definitely low altitude collisions, and Chirons are still fairly clean, the incoming binon may be one with a particularly low cross section for collisions with matter.

In this model, the apparent transverse momentum of most of the Chiron events is caused not by angular deviation at the collision, but instead by error induced by movement of the target with respect to the preferred reference frame. Despite the high transverse momentum, we expect the particle showers to be parallel, and, indeed, highly parallel, widely separated, particle showers is a characteristic of Centauros and Chirons.

If the binon manages to survive to the target, then an angle will be produced between the binon track and the normal particle showers. These should be rare, and in fact, there are few examples of Chirons or Centauros where there is an estimate of the collision height based on angular data. Note that the original triangulation data[53, 62] for the CentauroI event was retracted[63] in 2004.

The faulty CentauroI triangulation of 50±15m resulted in p_T of about 0.35GeV/c. This value was large, but seemed reasonable, and was used to estimate the heights of other Centauro and Chiron events.[53] Consequently, one is likely to see many estimates of heights of Centauro events in the earlier literature that should now be ignored.

In 1977, a balloon borne emulsion chamber was lucky enough to be hit by a Chiron close enough that it could be triangulated. This event was reanalyzed in 2001.[65] The result was that the apparent point from which the collision emanated was about 120 ± 40m above the chamber. The target was 100 nuclear emulsion layers, with a lead calorimeter. Estimated transverse momentum was 23 ± 7 GeV/c. The alignment parameter for the 4 highest energy particles was .9878, where 1 is perfect alignment. The spread in high energy particles was about 1.4cm.[65, Fig. 6]

The figures of 4cm and 120m allow us to reanalyze this event by attributing the apparent p_T to a preferred reference frame effect. Over a distance of 120 ± 40m, the time of flight for a c and a $3c$ particle will be 400 ± 130ns and 130 ± 44ns, respectively. The difference in arrival time will be 270 ± 90ns, so a separation of 1.4cm indicates a preferred reference frame velocity of 39 to 77km/s. This is low, but comparable with the average perpendicular preferred reference frame calculation of 150km/s. Unfortunately, the exposure time was 160 hours, so accurate information about the direction of the track, relative to the various purported preferred reference frames, is not available.

After disregarding the CentauroI triangulation, there are two other triangulation heights listed in [53]. CentauroVII which gave a height of 2000 to 3000m with a p_T comparable to CentauroI. ChironI gave a height of 330 ± 30m and p_T of 1.42GeV/c. The triangulation data is:

Event	Height(m)	$p_T(GeV/c)$
CentauroVII	2500 ± 500	0.35
ChironI	330 ± 30	1.42
Balloon1977	120 ± 40	23 ± 7

(77)

This is about what we expect for elastic binon collisions with respect to a preferred reference frame. The low triangulation data is generally more accurate and leads to higher estimates. We do not expect a binon, which should have a very large cross section, to survive a 2500m passage through the atmosphere.

B. High Transverse Momentum

Disregarding preferred reference frame effects, the p_T values for binon interactions should be higher than for standard quantum mechanics. Of the interactions in standard quantum mechanics, the only coupling between left and right handed particles consists of the mechanism that gives mass.

In the standard model, the various spin-1 forces apply to the leptons and quarks as a whole. This follows over to the binon model in that the vector bosons are coupled to the bound states of the binons. These forces, since they couple to bound states, use the spin of the bound state rather than the details of the individual binons. The usual forces can only couple between same handed states.

Binon theory treats mass as another force, one that binds together two chiral fermions into a single particle. Mass, as a force, is therefore unique in that it must treat the binons individually. Seen in this way, mass is a more fundamental force than the various forces mediated by vector bosons.

The high transverse momentum of mass treated as a force is seen in the zitterbewegung model of the electron. In this model, the electron is thought to travel at speed $\pm c$ as these are the only eigenvalues of the velocity operator in the Dirac equation. In this model, a stationary electron alternately moves back and forth at speed c, with its handedness reversing at each turning point. This results in an electron with an average position that is stationary, and with a consistent spin oriented in the direction of the movements. Thus the mass force is not only capable of completely reversing longitudinal momentum, but must do so constantly.

When this model is applied to binons, the fact that binons are travelling off axis relative to the electron implies that they intrinsically possess extremely high p_T, and reactions involving them, like the mass force itself, should be expected to have high p_T as well.

C. Tachyonic Precursors of Cosmic Ray Showers

If the primary particles in some cosmic rays are tachyons, it is only natural to expect that this will have an observable effect on how the shower evolves in time. It turns out that the effect will be quite small and difficult to observe.

Several attempts to explicitly find tachyons in cosmic rays have met with success[88, 89] or failure[90]. From the point of view of binons, a search of this sort will be rather difficult. Instead of surviving to the ground as a tachyonic particle, an individual binon will likely convert into quarks and leptons at high altitude.

Instead of a tachyonic precursor, at low altitude the time signature of a binon is likely to be a highly energetic air shower that has a duration somewhat longer than usual. If, between its first collision and its final one, the binon travels a distance of l meters at a speed of $3c$, the duration of the resulting air shower, at the core, will be extended by

$$\tau_{shower} = l(\frac{1}{c} - \frac{1}{3c}) = \frac{2\,l}{3c} \tag{78}$$

seconds. In addition, if there is a distance of l between consecutive collisions, there may be a corresponding time interval between consecutive peaks in the intensity of the shower.

The spread in time signature will be proportional to the distance between the binon's first collision and when it converts to regular matter. From the previous section, this should be around 100 meters. Accordingly, the air shower will be extended by about 200ns.

This time is barely within the ability of high energy cosmic ray experiments to register. For example, the HiRes experiment uses an analog to digital converter with a 100ns sampling period.[87] The Pierre Auger cosmic ray observatory has a better chance with a sampling rate of 40MHz for their Cherenkov detectors, and 100MHz for their air fluorescence telescopes.[91] The AGASA experiment uses photomultiplier tubes with the light intensity encoded as the logarithm of the pulse duration. The pulse corresponding to a single particle is 10 microseconds, so it is quite impossible for them to detect the duration of a air shower.[92]

While a typical shower might only be extended by 200ns, there will be some showers that are extended much longer. Since the AGASA encodes their light intensities by pulse duration, this could be the cause of their cosmic ray energy flux measurements being higher, and extending to higher energies as compared[93, Fig. 8] to the other cosmic ray observatories.

In cosmic rays, the time of arrival of hadrons is more precise than the arrival times of the electromagnetic particles, as the hadrons travel paths that are more straight. In showers that arrive at a shallower angle, the additional distance travelled through the atmosphere has the effect of stripping off the electromagnetic part of the shower. This leaves a tighter time signature. The signature time is probably short enough to detect a broadening due to a tachyonic primary particle with a survival distance long enough to generate the Centauro spreads.[91, Fig. 6]

D. Inelastic Binon Collisions

If we assume that extreme separation between mini-clusters is mostly due to preferred reference frame effects, the statistics for mini-cluster formation will give us information about the branching ratio for elastic binon collisions. After the binon is converted to quarks and leptons, we expect that the leptons will cascade in the manner predicted by the standard model, while the quarks will continue to exhibit anomalous behavior.

As opposed to binons, free quarks are understood by the standard model and are not likely to violate isospin

symmetry, so we can expect that the showers produced by free quarks will have both electromagnetic and hadronic portions. The extremely high energy of free quarks should give them high penetrative power. Both these effects are seen in mini-clusters.

The very large potential energy of free quarks should give them a larger than normal cross section, and exactly that is observed in mini-clusters. In addition, since color refers to an angle around the direction of propagation, we can expect free quarks to violate cylindrical symmetry, and therefore to have relatively high p_T collisions. This could be the explanation for the approximate 0.5GeV/c collisions seen.

Under the binon model, quarks are composed of a mixture of electron and neutrino binons. The electron and neutrino binons share the nondirectional parts of their idempotents but are distinguished by the directional parts. Therefore there is a coupling between these pairs of electron and neutrino binons.

Eventually, for energetic reasons, a free quark will take advantage of this coupling to convert to color-free matter. From that point on, the shower will lose its anomalous character and the standard model will take over.

E. Black Holes and Binons

Since binons travel at $3c$, they can penetrate the event horizon of a black hole. Since the conditions inside a black hole are expected to be extreme, and the only particles that can escape the black hole are tachyons, it is natural to suppose that black holes are binon factories.

Black holes are expected to form accretion disks. Binons emitted into the accretion disk will scatter and downconvert to normal matter. They will contribute to the heating of the accretion disk, but will not be observed at a distance.

The same transverse momentum effects that are seen in Centauro events, as well as heating in general, can be expected to knock normal matter out of the plane of the accretion disk. This will have the effect of thickening the accretion disk near the singularity. Only the regions near the axis of rotation of the black hole may be left open for binons to escape, and the thickening of the accretion disk may leave the angles available for binons to escape to be small. Later, when the binons impact matter at some distance to the black hole, they will produce collimated particle showers that will appear as jets to distant observers.

We can expect that the region open for binons to escape will not always be exactly aligned with the black hole spin axis, and so the surviving particle showers will change in direction and opening angle. Since the occlusion may happen near the throat of the black hole, we can expect to see changes in jet strength and direction at rates suitable to the size of the black hole.

Any binons that escape the region of the black hole unconverted to normal matter will continue travelling. At the same time, visible radiation and light will be generated by the binons who were not so lucky.

The difference in speed between the binons and the associated particle shower debris is quite large. Consequently, even if we have very good data on the direction of the source of the binon, and even if the binon is uncharged and so is undeflected by magnetic fields, it may be difficult or impossible to match the binon up with a visible source. This is due to several effects. First, the black hole could have begun radiating so recently that no radiation of speed c could have reached us. Second, motion of the black hole could cause its apparent position at the time of arrival of the two signals to be displaced.

Finally, even if the black hole radiates continuously and is not moving, our own proper motion with respect to the preferred reference frame will cause the apparent directions of the black hole, as determined by radiation with speed c and its direction as determined by radiation with speed $3c$ radiation to diverge. This effect will be comparable in angle to about $v/c = 2.0 \times 10^5/3 \times 10^8 = 0.0007$ radians.

This effect, that is, that the binons from a black hole could reach us before normal matter and energy, suggests that when we use ancient photons to look for sources of high energy cosmic rays, we should consider the possibility that the photons are providing an obsolete description. Thus we should not be too surprised to see binons emitted from a direction in which a black hole has not yet appeared. Instead, we should look for evidence that a black hole is likely to form there "in the future".

F. Gamma-ray Bursts and Binons

Since gamma-ray bursts have been associated with black holes and jets, there is likely a connection to binons. That is, gamma rays may be the remains of particle showers produced by binons created by black holes. We imagine that a sudden influx of matter into a black hole, or perhaps the initial formation of the black hole in a supernovae, will create a burst of binons that then interact with nearby matter to create particle showers that we eventually observe as gamma ray bursts.

As mentioned in the previous subsection, the difference in propagation delay between photons and binons, over interstellar distances, will eliminate any observable time correlation between binon cosmic rays and the associated gamma ray bursts. However, if the particle showers are created over an extended region near the black hole, there will be a corresponding spread in arrival time of the debris from the associated showers.

First, as was noted in Subsec. (III C) particle showers induced by single particles in the atmosphere naturally spread in time, quite apart from any tachyonic effects, on the order of 1 to 10 microseconds. Gamma ray bursts, by comparison, have typical durations around 10 to 100 seconds, around 10^7 times longer. Perhaps the density of the media in which binons produce gamma ray bursts is

about 10^{-7} that of the atmosphere.

Gamma ray bursts are often accompanied by nonthermal precursors 10 to 200 seconds ahead of the main burst with about 1% of the energy.[75] If a small percentage of the binons emitted at the black hole were to penetrate the region where most of the gamma rays were produced, and then were to encounter matter in a region around 6 to 60×10^9 meters away, the result would be a precursor with the appropriate delay.

The effect of jets emitted by a black hole would be to sweep matter away from the axis of the black hole. This could clear the way for later binon bursts to postpone showering until they reached the end of the empty region. This mechanism could produce delayed gamma ray bursts that are created from the difference in travel time of radiation created in the main shower media and radiation created at the inner edge of the accretion disk.

G. Velocity Eigenstates of Binons

It is customary, in the standard model of QM, to analyze particle interactions in the momentum representation. In the momentum representation, energy and momentum are naturally conserved, but particle positions are not. The position representation, while losing energy and momentum conservation, is a natural representation for a theory that must take into account positions in the hidden dimension.

If one assumes a Lorentz symmetric world, then it is natural that a model of one photon at some specific energy would imply the existence of a continuum of models of photons at various other energies.

A scheme, such as the present one, that assumes a preferred reference frame does not have this natural method of assigning various energies to a single massless particle type. Since there is a preferred reference frame, an electron travelling at one speed can be distinguished, in principle, from an electron travelling at some other speed. Similarly, a photon or binon travelling with one energy level can be distinguished from the same particle travelling at energy. This leads to a question of how it comes about that two identical massless particle can possess different energies and still be identical.

A solution is to assign a "bare" propagator that is a velocity eigenstate to represent a particle, and then to obtain effective propagators for the various possible momenta and energy through a resummation. One then obtains the quantum mechanics of the standard particles as an effective field theory from a very simple but unusual underlying field theory.

These bare propagators do not correspond to any specific energy or momenta. This is a natural extension of the zitterbewegung model of the electron to massless particles composed of chiral fermions.

The application to astrophysics has to do with black holes. Since the black hole event horizon is fundamentally a velocity barrier, rather than a momentum barrier, it could be that the proper way of classifying the binons that escape a black-hole is in their velocity eigenstates rather than their momentum eigenstates.

Massless particles in velocity eigenstates do not carry specific momenta or energy. Instead, if one carries out an energy measurement of such a particle, one obtains a set of possible values according to a probability density.

Since the energy deposited by a binon in standard matter will largely depend on the number of collisions that the binon survives before converting to standard matter, we can model the energy content of a binon velocity eigenstate by assuming a model based on a Poisson process.

If we assume that each elastic collision deposits an energy E_0, and that the binon survives unaltered with probability p, then the spectrum of energies deposited by the binon will follow the probability density:

$$\rho(nE_0) = p^n = (p^{1/E_0})^{nE_0}. \tag{79}$$

Replacing nE_0 with E, multiplying by E^3 and converting to logarithms gives a form compatible with Fig. (9):

$$\log(E^3\,\rho) = \log(\rho_0) + 3\log(E/E_0) - 10^{\log(E/E_0)}. \tag{80}$$

For small values of E, the second term dominates, and will give a fairly steep positive slope of 3. For large values of E, the last term dominates and will give an even steeper drop off.

At this time, even the simplest fact about high energy cosmic rays, namely their energy spectrum, is uncertain.[93] Fitting the above curve to the data requires knowledge of both the energy flux of cosmic rays and their composition, so we will refrain from attempting a fit of the above curve to the data.

H. Binon / Tachyon Cosmology

Since tachyons would dominate the early universe, they would allow parts of the universe that could not be in communication by light limited particles to come to equilibrium. This result is a natural inflation that is useful in cosmology.[94–97] Other writers suggest tachyons as an explanation for dark matter or energy.[98, 99]

APPENDIX A: CLASSICAL SPECIAL RELATIVITY CALCULATIONS IN PTG

In order to make clear how classical calculations in the PTG can match those of special relativity, this appendix provides detailed calculations for time dilation and length contraction using both techniques.

1. Time Dilation

Problem: A spaceship travels 3 light years away form earth, at a speed of $0.6c$, and then returns at the same

speed. What is the proper time experienced on the Earth during the voyage, and what is the proper time experienced on the spaceship?

Special Relativity Solution: The voyage requires 3/0.6 = 5 years each way for a total of 10 years. This is the proper time experienced on the Earth. The spaceship experiences a time dilation of $(1 - 0.6^2)^{0.5} = 0.8$, so the proper time experienced on the spaceship is $10 \times 0.8 = 8$ years.

PTG Solution: The spaceship starts at the point $(x, y, z, s) = (0, 0, 0, 0)$. Align the x axis with the direction of travel. The velocity of the spaceship on the outgoing voyage is therefore given by the vector $(0.6, 0, 0, 0.8)$. The 0.8 value is required to make the speed of the spaceship work out in total be 1. The spaceship's position as a function of the global time t is therefore:

$$(0, 0, 0, 0) + (0.6, 0, 0, 0.8)t_1 \tag{A1}$$

Setting this equal to $(3, 0, 0, s_1)$ gives t_1, the global coordinate time for the arrival of the spaceship at its destination, and t_1 is therefore 5 years. Note that the value of s_1 is unspecified, as the total length of the hidden dimension is negligible as compared to the many light years of travel. Since the proper time component of the velocity of the spaceship is 0.8, the total elapsed proper time on the outgoing voyage of the spaceship is therefore $0.8 \times 5 = 4$ years. Similarly, the return trip uses a velocity of $(-0.6, 0, 0, 0.8)$ and results in a coordinate time passage of 5 years and a proper time for the spaceship of another 4 years. The result is, of course, identical to the Special Relativity result.

2. Lorentz Contraction

A rod flies lengthwise through a laboratory with a speed of $0.923c$. The lab measures the length of the rod as 6 meters. How long is the rod measured in a coordinate system moving with the rod?

Special Relativity Solution: The Lorentz contraction factor is $(1 - 0.923^2)^{-0.5} = 2.6$, so the proper length of the rod is $6m \times 2.6 = 15.6$ meters.

In any given coordinate system, the constancy of the speed of light provides a technique for measuring length. Accordingly, the rod can be measured in its own frame of reference by calculating the time required for light to travel the length of the rod. Since proper time is a property of individual particles, rather than dimensional objects such as rods, the length of the rod will have to be measured by computing the time required for the light to travel down the rod, be reflected at the end, and then travel back to the point of origin on the rod. The proper time experienced by the end point of the rod during this flight will indicate (when multiplied by c) twice the length of the rod.

So let the rod begin at position $(0, 0, 0, 0)$ through $(6m, 0, 0, 0)$, and set the velocity vector for the rod to be $(0.923, 0, 0, 0.384)$ so that it moves in the $+x$ direction. The light signal starts at $(0, 0, 0, 0)$ and proceeds with a velocity vector of $(1, 0, 0, 0)$ until it meets with the other end of the bar at time t_1. The light direction is then reversed, and it travels with velocity $(-1, 0, 0, 0)$ until it meets up with the trailing end of the bar at time t_2. The length of the bar, in the reference frame of the bar, is then 1/2 the proper time experienced by the trailing end of the bar from 0 to t_2. The equations for t_1 and t_2 are therefore:

$$\begin{aligned} (0,0,0,0) &+ (1,0,0,0)t_1 \\ = (6,0,0,0) &+ (0.923,0,0,0.384)t_1, \qquad \text{(A2)} \\ (1,0,0,0)t_1 &+ (-1,0,0,0)(t_2 - t_1) \\ = (0,0,0,0) &+ (0.923,0,0,0.384)t_2. \qquad \text{(A3)} \end{aligned}$$

Since our world does not distinguish between the hidden s coordinate, the equalities need only be established for the first three coordinates.

The solution is $t_1 = 78$ meters, and $t_2 = 81.12$ meters. The proper time experienced on the trailing edge of the rod is, by time dilation, 0.384 of t_2, which gives 31.2. Half of this is the proper length of the bar, which is the same as the value given by special relativity. Therefore, both theories show the Lorentz contraction of the bar to be the same. Since the two theories are the same in both time dilation and Lorentz contraction, any dynamical problem can be converted between them, and the results of standard relativity translate directly. Thus the problem can be worked with the simpler methods of SR with only a philosophical difference.

APPENDIX B: SCHWINGER MEASUREMENT ALGEBRA

Following Julian Schwinger's 1955 lectures onquantum kinematics[100, Chap. 1.1], but specializing to the case of the electron fermion family, let A denote a set of characteristics that distinguish the 32 particles in a family $\mathcal{F}$ of elementary fermions. We will define the QCD colors as $\{1, 2, 3\}$, and use the following designations for such a family:

$$\begin{aligned} \mathcal{F} = \quad & \{e_L, e_R, \bar{e}_L, \bar{e}_R, \nu_L, \nu_R, \bar{\nu}_L, \bar{\nu}_R, \\ & u_{1L}, u_{1R}, \bar{u}_{1L}, \bar{u}_{1R}, u_{2L}, u_{2R}, \bar{u}_{2L}, \bar{u}_{2R}, \\ & u_{3L}, u_{3R}, \bar{u}_{3L}, \bar{u}_{3R}, d_{1L}, d_{1R}, \bar{d}_{1L}, \bar{d}_{1R}, \\ & d_{2L}, d_{2R}, \bar{d}_{2L}, \bar{d}_{2R}, d_{3L}, d_{3R}, \bar{d}_{3L}, \bar{d}_{3R}\} \end{aligned}$$

Let a_1 be an elementary particle in $\mathcal{F}$. Let $M(a_1)$ symbolize the selective measurement that accepts particles of type a_1, and rejects all others. One can imagine some sort of Stern-Gerlach apparatus, though since quarks are apparently permanently bound it will have to be an imaginary apparatus. We can define addition of measurements to be the less selective measurement that accepts particles of any of the included types:

$$M(a_1) + M(a_2) = M(a_1 + a_2). \tag{B1}$$

Two successive measurements can be represented by multiplication of the measurement symbols. Because of the physical interpretations of the symbols, addition is associative and commutative, while multiplication is at least associative. One and zero represent the trivial measurements that accept all or no particles. Clearly, $0 + M(a^1) = M(a^1)$, $1M(a^1) = M(a^1)1 = M(a^1)$, and $0M(a^1) = M(a^1)0 = 0$, so the set of measurements form an algebra. The "elementary" measurements associated with these 32 fermions satisfy the following equations:

$$M(a^1)M(a^1) = M(a^1), \tag{B2}$$

$$M(a^1)M(a^2) = 0, a^1 \neq a^2, \tag{B3}$$

$$\sum_{n=1}^{n=32} M(a^n) = 1 \tag{B4}$$

Schwinger goes on to analyze incompatible measurements, such as spin in two different directions, but these simple results are enough to establish the similarity to the approach of the present paper.

APPENDIX C: THE LOUNESTO GROUP

Other than $\hat{1}$, the remaining 31 canonical basis elements have eigenvalues of -1 as well as $+1$. The multiplicity of each is sixteen, and the eigenvectors are easy to write down. For example, the eigenvectors of $\widehat{xyt}$ with eigenvalue -1 are given by:

$$\widehat{xyt}(1 - \widehat{xyt})\eta = -(1 - \widehat{xyt})\eta, \tag{C1}$$

where η is any Clifford algebra constant that doesn't annihilate $(1 - \widehat{xyt})$. Sixteen values for η that give linearly independent eigenvectors include any nonzero term in the product $(1 + \hat{x} + \hat{y} + \hat{t})(1 + \hat{z})(1 + \hat{s})$.

Clifford algebra elements of the form $(1 \pm e)/2$ are idempotent, if e is any element that gives 1 when squared. If e_1, e_2 and e_3 mutually commute and square to 1, then

$$\iota = (1 \pm e_1)(1 \pm e_2)(1 \pm e_3)/8, \tag{C2}$$

where the $\pm$ are to be taken independently, are eight idempotents. If e_1, e_2, and e_3 are canonical basis elements and generate a group of size 8 under multiplication, then these eight idempotents are distinct, and in the context of the Clifford algebra used here, are mutually annihilating primitive idempotents.[101] An example of a set of e that satisfy these requirements is $e_1 = \widehat{zt}$, $e_2 = \widehat{ixy}$, $e_3 = \hat{s}$.

Out of respect for the contributions of Pertti Lounesto to the mathematical understanding of spinors, we will refer to a set of e_n that satisfy these requirements:

$$\begin{aligned} e_n e_m &= e_m e_n, \\ e_n &\in \text{Canonical basis}, \\ e_n^2 &= 1, \\ \{e_n\}_{n=1}^3 &\quad \text{generates a group of order 8,} \end{aligned} \tag{C3}$$

as a set of "Lounesto group generators". The group of size 8 will then be the "Lounesto group".

Since the Lounesto group generators commute, so do their various products. Therefore Eq. (C2) gives primitive idempotents that possess good quantum numbers with respect to all eight Lounesto group elements. Seven of the Lounesto group elements are nontrivial, the trivial one is 1.

The choice of generators among the Lounesto group is somewhat arbitrary. So long as we pick three group elements that are distinct and nontrivial, and we avoid picking a set that multiplies to unity, our three elements will generate the other five. Translated back into physics, this means that we need only keep track of three quantum numbers for each of the primitive idempotents. The rest are related by multiplication.

[1] D. Hestenes, *Space Time Algebra* (Gordon and Breach, New York, 1966).
[2] L. de Broglie, Comptes Rendus **177**, 507 (1923).
[3] K. W. Ford, *Classical and Modern Physics, Volume 3* (Wiley, 1974).
[4] K. Krogh, *Gravitation without curved space-time* (2004), astro-ph/9910325.
[5] A. Messiah, *Quantum Mechanics, Vol I* (John Wiley and Sons, 1958).
[6] M. E. Peskin and D. V. Schroeder, *An Introduction to Quantum Field Theory* (Addison-Wesley Publishing Company, 1995).
[7] J. M. C. Montanus, *Proper-Time Formulation of Relativistic Dynamics*, Found. Phys. **31**, 1357 (2001).
[8] A. Gersten, *Euclidean Special Relativity*, Found. of Phys. **33**, 1237 (2003).
[9] J. B. Almeida, *Euclidian formulation of general relativity*, `http://www.arxiv.org/abs/math.GM/0406026` (2004).
[10] J. B. Almeida, *The null subspaces of G(4,1) as source of the main physical theories*, `http://www.arxiv.physics/0410035` (2004).
[11] A. Lasenby, C. Doran, and S. Gull, *Gravity, Gauge Theories and Geometric Algebra*, Phil. Trans. R. Lond. **A 356**, 487 (1998).
[12] D. Hestenes, *Spacetime geometery with geometric calculus.*
[13] S. Setiawam, *Applications of geometric algebra to black holes and Hawking radiation* (2004), physics/0412070.
[14] J. Lindesay and T. Gill, *Canonical proper time formulation for physical systems.*
[15] T. Gill and W. Zachary, Found. Phys. **31**, 1299 (2001).

[16] T. Gill and J. Lindesay, Int. J. Theoretical Phys. **32**, 2087 (1993).

[17] M. Herrero, *The standard model* (1998), hep-ph/9812242.

[18] J. Ryan, *Lectures on Clifford (Geometric) Algebras and Applications* (Birkhauser, 2004).

[19] W. M. P. Jr. and J. J. Adams, *Should metric signature matter in Clifford algebra formulations of physical theories?* (1997), gr-qc/9704048.

[20] C. A. Brannen, *The geometry of fermions*, `http://www.brannenworks.com/a_fer.pdf` (2004).

[21] P. Lounesto, *Clifford Algebras and Spinors* (Cambridge University Press, 1997).

[22] K. Huang, *Quarks, Leptons and Gauge Fields* (World Scientific Publishing, 1982).

[23] H. Harari, *A schematic model of quarks and leptons*, SLAC-PUB-2310 (1979).

[24] E. Ma, *Triplicity of quarks and leptons* (2005), hep-ph/0502024.

[25] B. Schmeikal, *Minimal Spin Gauge Theory - Clifford Algebra and Quantumchromodynamics*, Advances in Applied Clifford Algebras **11 No. 1**, 63 (2001).

[26] M. Pavsic, *Kaluza-Klein theory without extra dimensions: Curved Clifford space* (2005), hep-th/0412255.

[27] T. Smith, *From sets to quarks: Deriving the standard model plus gravitation* (1998), hep-ph/9708379.

[28] D. Hestenes, *New Foundations for Classical Mechanics* (Kluwer Academic Publishers, 1999).

[29] M. Francis and A. Kosowsky, *Geometric algebra techniques for general relativity* (2004), gr-qc/0311007.

[30] J. B. Almeida, *Standard-model symmetry in complexified spacetime algebra*, `http://www.arxiv.org/abs/math.GM/0307165` (2003).

[31] I. G. Avramidi, *Dirac operator in matrix geometry* (2005), math-ph/0502001.

[32] D. Hestenes, *Real Spinor Fields*, J. Math. Anal. and Appl. **8**, 798 (1967).

[33] A. Messiah, *Quantum Mechanics, Vol II* (John Wiley and Sons, 1958).

[34] H. Sato, *Invisible un-removable field: A search by ultra-high energy cosmic rays* (2003), astro-ph/0311306.

[35] G.-J. Ni, *Cosmic ray spectrum and tachyonic neutrino* (2004), hep-ph/0404030.

[36] J. Rembielinski, *Superluminal phenomena and the quantum preferred frame* (2000), quant-ph/0010026.

[37] T. Jacobson, S. Liberati, and D. Mattingly, *Lorentz violation at high energy: Concepts, phenomena and astrophysical constraints* (2005), astro-ph/0505267.

[38] S. L. Glashow, A. Halprin, P. I. Krastev, C. N. Leung, and J. Pantaleone, *Comments on neutrino tests of special relativity* (1997), hep-ph/9703454.

[39] D. Mattingly, *Modern tests of Lorentz invariance* (2005), gr-qc/0502097.

[40] S. Mukohyama, *Ghost condensation and gravity in Higgs phase* (2005), hep-th/0505080.

[41] T. Chang and G. Ni, *An explanation of negative mass-square of neutrinos* (2000), hep-ph/0009291.

[42] E. Recarni, *Superluminal motions? a bird-eye view of the experimental situation* (2001), physics/0101108.

[43] Z. C. Tu and Z. Y. Wan, *The development of special relativity in the superluminal case* (2001), physics/0107032.

[44] R. Qi, *Space-time transformation for superluminal signaling* (2002), 0210021.

[45] M. Consoli and E. Costanzo, *The motion of the solar system and the Michelson-Morley experiment* (2003), astro-ph/0311576.

[46] J. Gervais and J. Roussel, *Solving the strongly 2D gravity: 2. fractional-spin operators, and topological three-point functions.* (1994), hep-th/9403026.

[47] C. A. Brannen, *The geometric speed of light*, `http://www.brannenworks.com/a_tgsol.pdf` (2004).

[48] J. C. Yoon, *Lorentz violation of the standard model* (2005), hep-ph/0502142.

[49] R. Hatch, *Those Scandalous Clocks*, GPS Solutions **8**, 67 (2004).

[50] A. Unzicker, *What can physics learn from continuum mechanics?* (2000), gr-qc/0011064.

[51] P. Bhattacharjee and G. Sigl, *Origin and propagation of extremely high energy cosmic rays* (1999), astro-ph/9811011.

[52] F. W. Stecker, *Cosmic physics: The high energy frontier* (2003), astro-ph/0309027.

[53] E. Gladsyz-Dziadus, *Are Centauros exotic signals of the QGP?*, Institute of Nuclear Physics, Krakow, Report No. 1879/PH (2001), hep-ph/0111163.

[54] F. Halzen, *FELIX: The cosmic ray connection.*

[55] R. Engel, *Very high energy cosmic rays and their interactions* (2005), astro-ph/0504358.

[56] M. Martinis, V. Mikuta-Martinis, A. Svarc, and J. Crnugelj, *Isospin correlations in high-energy heavy-ion collisions* (1995), hep-ph/9501210.

[57] M. M. Aggarwal and WA98Collaboration, *Localized charged-neutral fluctuations in 158 A GeV Pb+Pb collisions* (2000), nucl-ex/0012004.

[58] J. D. Bjorken, K. L. Kowalski, and C. C. Taylor, *Observing disoriented chiral condensates* (1993), hep-ph/9309235.

[59] S. Barshay and G. Kreyerhoff, *Are neutral Goldstone bosons initiating very energetic air showers and anomalous multiple-core structure as a component of cosmic rays?* (2004), hep-ph/0005022.

[60] X. U. Renxin and W. U. Fei, *Ultra high energy cosmic rays: Strangelets?* (2003), astro-ph/0212103.

[61] A. Mironov and A. Morozov, *Can Centauros or Chirons be the first observations of evaporating mini black holes?* (2004), hep-ph/0311318.

[62] C. M. G. Lattes and etal (Japan-Brasil collaboration), *Proceedings of the 13th International Cosmic Ray Conference*, **3**, 2227 (1973).

[63] A. Ohsawa, E. H. Shibuya, and M. Tamada, *The exotic characteristics of Centauro-1 re-examination of the Centauro event* (2004).

[64] A. Borisov, V. Maximenko, R. A. Mukhamedshin, V. Puchkov, and S. A. Slavatinsky, *Coplanar Production of Pions at Energies above 10 PeV According to Pamir Experiment Data*, International Cosmic Ray Conference **28**, 85 (2003).

[65] V. I. Osedlo, I. V. Rakobolskaya, V. I. Galkin, A. K. Managadze, L. G. Sveshnikova, L. A. Goncharova, K. A. Kotelnikov, A. G. Martynov, and N. G. Polukhina, *A superfamily with $\Sigma E_\gamma > 10^{15}$ eV observed in stratosphere*, Proceedings of ICRC 2001 p. 1426 (2001).

[66] V. V. Kopenkin, A. K. Managadze, I. V. Rakobolskaya, and T. M. Roganova, *Alignment in gamma-hadron families of cosmic rays* (1994), hep-ph/9408247.

[67] M. Pohl, W. Reich, T. P. Krichbaum, K. Standke, S. Britzen, H. P. Reuter, P. Reich, R. Schlickeiser, R. L. Fiedler, E. B. Waltman, et al., *Radio observations of the*

γ-ray quasar 0528+134 superluminal motion and an extreme scattering event (1995), astro-ph/9503082.

[68] S. G. Jorstad and A. P. Marscher, *The highly relativistic kiloparsec-scale jet of the gamma-ray quasar 0827+243* (2004), astro-ph/0405424.

[69] C. M. Urry, *Unified schemes for radio-loud active galactic nuclei* (1995), astro-ph/9506063.

[70] C. M. Urry, *An overview of blazar variability* (1996), astro-ph/9609023.

[71] K. I. Kellermann, M. L. Lister, D. C. Homan, E. Ros, J. A. Zensus, M. H. Cohen, M. Russo, and R. C. Vermeulen, *Superluminal motion and relativistic beaming in blazar jets* (2002), astro-ph/0211398.

[72] I. F. Mirabel and L. F. Rodriguez, *Sources of Relativistic Jets in the Galaxy*, Annu. Rev. Astron. Astrophys. **37**, 409 (1999).

[73] M. Massi, M. Ribo, J. M. Paredes, S. T. Garrington, M. Peracaula, and J. Marti, *The gamma-ray emitting microquasar LSI+61 303* (2004), astro-ph/0410504.

[74] J. I. Katz, *Delayed hard photons from gamma-ray bursts* (1994), astro-ph/9405033.

[75] D. Lazzati (2004), astro-ph/0411753.

[76] T. Stanev, R. Engel, A. Mucke, R. J. Protheroe, and J. P. Rachen, *Propagation of ultra-high energy protons in the nearby universe* (2000), astro-ph/0003484.

[77] L. Anchordoqui, H. Goldberg, S. Reucroft, and J. Swain, *Extragalactic sources for ultra high energy cosmic ray nuclei* (2001), hep-ph/0107287.

[78] A. Mattei, *Ultra high energy cosmic rays from charged black holes.* (2005), astro-ph/0505616.

[79] S. Coleman and S. L. Glashow, *Cosmic ray and neutrino tests of special relativity* (1997), hep-ph/9703240.

[80] D. Rohrlich and Y. Aharonov, *Cherenkov radiation and superluminal particles* (2002), quant-ph/0107025.

[81] L. Gonzalez-Mestres, *Superluminal particles and high-energy cosmic rays* (1997), physics/9705032.

[82] L. Gonzalez-Mestres, *Lorentz symmetry violation and superluminal particles at future colliders* (1997), physics/9708028.

[83] F. W. Stecker and S. T. Scully, *Lorentz invariance violation and the spectrum and source power of ultrahigh energy cosmic rays* (2005), astro-ph/0412495.

[84] G. R. Farrar and P. L. Biermann, *Correlation between Compact Radio Quasars and Ultra-High Energy Cosmic Rays*, Phys. Rev. Lett. **81**, 3579 (1998).

[85] G. R. Farrar and P. L. Biermann, *Reply to comment on correlation between cosmic radio quasars and ultra-high energy cosmic rays* (1999), astro-ph/9901315.

[86] S. Sarkar, *New physics from ultrahigh energy cosmic rays* (2003), hep-ph/0312223.

[87] R. U. Abbasi, T. Abu-Zayyad, J. F. Amman, G. C. Archbold, J. A. Bellido, K. Belov, J. W. Belz, D. R. Bergman, Z. Cao, R. W. Clay, et al., *Monocular measurement of the spectrum of UHE cosmic rays by the FADC detector of the HiRes experiment* (2004), astro-ph/0208301.

[88] F. Ashton, J. Fatemi, H. Nejebat, A. Nasri, W. S. Rada, E. Shaat, A. C. Smith, T. R. Stewart, M. G. Thompson, and M. W. Treasure, *Preliminary results of a search for faster than light objects in cosmic rays at sea level*, International Cosmic Ray Conference **7**, 370 (1978).

[89] V. D. Ashitkov, T. M. Kirina, A. P. Klimakov, R. P. Kokoulin, and A. A. Petrukhin, *Investigation of advance particles from the viewpoint of the tachyon hypothesis*, Bull. of Acad. of Sci. USSR Phys. pp. 153–155 (1985).

[90] G. R. Smith and S. Standil, *Search for tachyons preceeding cosmic ray extensive air showers with energy greater than about 10 to the fourteenth eV*, Canadian Journal of Physics **55**, 1280 (1977).

[91] K. H. Kampert and Pierre Auger Collaboration, *The Pierre Auger observatory – status and prospects –* (2005), astro-ph/0501074.

[92] M. Takeda, N. Salaki, K. Honda, M. Chikawa, M. Fukushima, N. Hayashida, N. Inoue, K. Kadota, F. Kakimoto, K. Kamata, et al., *Energy determination in the Akeno giant air shower array experiment*, astro-ph/0209422.

[93] R. U. Abbasi, T. Abu-Zayyad, J. F. Amman, G. Archbold, R. Atkins, J. A. Bellido, K. Belov, J. W. Belz, S. Y. B. Zvi, D. R. Bergman, et al., *Observation of the ankle and evidence for a high-energy break in the cosmic ray spectrum* (2005), astro-ph/0501317.

[94] G. W. Gibbons, *Thoughts on tachyon cosmology* (2003), hep-th/0301117.

[95] X. zhou Li and X. hua Zhai, *The tachyon inflationary models with exact mode functions* (2003), hep-ph/0301063.

[96] S. Nojiri and S. D. Odintsov, *Effective equation of state and energy conditionts in phantom/tachyon inflationary cosmology perturbed by quantum effects* (2003), hep-th/0306212.

[97] J. S. Bagla, H. K. Jassal, and T. Padmanabhan, *Cosmology with tachyon field as dark energy* (2003), astro-ph/0212198.

[98] P. F. Gonzalez-Diaz, *Dark energy and supermassive black holes* (2004), astro-ph/0408450.

[99] P. C. W. Davies, *Tachyonic dark matter* (2004), 0403048.

[100] J. Schwinger, *Quantum Kinematics And Dynamics* (Perseus Publishing, 1991).

[101] P. Lounesto, *Scalar Products of Spinors and an Extension of Brauer-Wall Groups*, Found. Phys. **11**, 721 (1981).